CUKUROVA UNIVERSITY

INSTITUTE OF NATURAL AND APPLIED SCIENCES

MSc THESIS

# Validating A Test Method To Evaluate The Adhesion Force of Electrospun Nanofiber Covered Nitinol Stents and Evaluating The Adhesion Force Of Differently Treated Stents

**Md Abul SHAHID**

*Textile Engineering Department*

September, 2023

**CONTENTS**

**CUKUROVA UNIVERSITY**
**INSTITUTE OF NATURAL AND APPLIED SCIENCES**

**MSc THESIS**

# Validating A Test Method To Evaluate The Adhesion Force of Electrospun Nanofiber Covered Nitinol Stents and Evaluating The Adhesion Force Of Differently Treated Stents

**Md Abul SHAHID**

***Advisor: Prof. Dr. Osman BABAARSLAN***

***Department of Textile Engineering***

## ABSTRACT

The main objective of this study is to measure the adhesion force between braided structured nitinol stent's surface and thermoplastic polyurethane (TPU) electrospun nanofibers. Further, the influence of different treatments on the adhesion force should be investigated, and a method to enhance adhesion should be found. To measure the adhesion force of TPU nanofiber covered stents, first, a method was validated using different surface materials and adhesives. After that test method validation, the adhesion force is measured. Later, different approaches are followed to evaluate the adhesion force, such as different electrospinning processes, braided structures, and treatments. From the validation part, it has been observed that the adhesion forces of 2D and 3D surfaces are quite coherent and reproducible. Similar results have been found for 2D, and 3D structured nanofiber covered stents. In terms of different approaches, higher adhesion forces have been observed for horizontal electrospinning setups and braided structures with higher forwarding speeds. After plasma treatment, adhesion forces were increased by 2 times, while for heat treatment, it was increased by 1.5 times. The average adhesion force of the stent after plasma and heat treatment was 41.8 cN and 26.41 cN, respectively, while the reference stent without treatment measured 16.75 cN.

**Keywords**: nitinol stents, electrospun nanofiber, adhesion force, test method validation

**ÇUKUROVA ÜNİVERSİTESİ**
**FEN BİLİMLERİ ENSTİTÜSÜ**

**YÜKSEK LİSANS TEZİ**

# Elektrospun Nanofiber Kaplanacak Nitinol Stentlerde Yapışma Durumunun Değerlendirilmesi İçin Yeni Bir Test Metodu ve Yapışmayı Artırma Yönteminin Geliştirilmesi

**Md Abul SHAHID**

***Danışman: Prof. Dr. Osman BABAARSLAN***

***Tekstil Mühendisliği Anabilim Dalı***

## ÖZ

Bu çalışmanın temel amacı, örgülü yapılı nitinol stentin yüzeyi ile termoplastik poliüretan (TPU) elektrospun nanolifler arasındaki yapışma kuvveti araştırılmıştır. Ayrıca, farklı işlemlerin adezyon kuvveti üzerindeki etkisi araştırılmış ve adezyonu artıracak bir yöntem bulunmaya çalışılmıştır. TPU nanofiber kaplı stentlerin yapışma kuvvetini ölçmek için öncelikle farklı yüzey malzemeleri ve yapıştırıcılar kullanılarak bir yöntemin doğrulaması yapılmıştır. Bu test yöntemi doğrulamasından sonra, yapışma kuvveti ölçülmüştür. Daha sonra, farklı elektrospinning işlemleri, örgülü yapılar ve işlemler gibi yapışma kuvvetini değerlendirmek için farklı yaklaşımlar izlenmiştir. Doğrulama kısmında, 2D ve 3D yüzeylerin yapışma kuvvetlerinin oldukça tutarlı ve tekrarlanabilir olduğu gözlemlenmiştir. 2D ve 3D yapılı nanofiber kaplı stentler için benzer sonuçlar bulunmuştur. Farklı yaklaşımlar açısından, yatay elektroeğirme kurulumları ve daha yüksek iletme hızlarına sahip örgülü yapılar için daha yüksek yapışma kuvvetleri gözlemlenmiştir. Plazma işleminden sonra adezyon kuvvetleri 2 kat, ısıl işlemden sonra ise 1,5 kat artmıştır. Plazma ve ısıl işlemden sonra stentin ortalama yapışma kuvveti sırasıyla 41.8 cN ve 26.41 cN iken, işlem görmemiş referans stentin yapışma kuvveti 16.75 cN ölçülmüştür.

**Anahtar Kelimeler**: Nitinol stentler, elektrospun nanolif, adezyon kuvveti, test yöntemi doğrulama

## EXTENDED ABSTRACT

Heart disease, including blocked or narrowed blood vessels, is a leading cause of death worldwide. According to the World Health Organization (WHO), cardiovascular disease is responsible for 17.9 million deaths per year, accounting for 31% of all global deaths. Coronary artery disease, which is caused by the buildup of plaque in the coronary arteries, is a major form of cardiovascular disease and is responsible for 7.4 million deaths per year. Stents are frequently used for cardiovascular diseases. A stent is a medical device that is used to treat narrowed or blocked blood vessels. It is a small, expandable tube that is inserted into a blood vessel to hold it open and improve blood flow. Stents are most commonly used to treat conditions such as atherosclerosis, a buildup of plaque on the inner walls of the arteries, and to prevent restenosis, the re-narrowing of a blood vessel after angioplasty. Different types of stents are available among them covered stents has lot of potentiality that has a material covering its length and circumference by using different kinds of materials. Covered stents are a viable alternative to surgery for the exclusion of coronary aneurysms and may have a function in the treatment of friable embolization-prone plaques.

Nanofiber covered stents are a type of stent that have a coating of electrospun nanofibers on their surface. Electrospinning is a process used to produce very fine fibers from polymer solutions or melts. The process involves the use of an electric field to draw charged polymer droplets or streams into fibers with diameters that can range from tens of nanometers to several micrometers. The resulting fibers have a high surface area-to-volume ratio, which makes them useful in a wide range of applications, including filtration, tissue engineering, and drug delivery. The nanofibers used to coat stents are typically made from biodegradable polymers such as polylactic acid (PLA) or polycaprolactone (PCL).

The main advantage of using nanofiber coatings on stents is that they can provide a controlled release of drugs to the site of the stent placement. This can help to prevent restenosis, which is the re-narrowing of a blood vessel after angioplasty. The drugs are incorporated into the nanofibers during the electrospinning process and are released over time as the fibers degrade. Nanofiber coatings can also improve the biocompatibility of stents by providing a surface that is less prone to causing inflammation or blood clots. Additionally, the small size of the fibers can make the surface of the stent more porous, which can improve the ability of the stent to promote tissue growth and healing.

Nanofiber-coated stents are still in the research and development phase, they have not yet been approved for use in the clinical setting, but they have shown promising results in animal studies and in vitro testing. Overall, Nanofiber coated stents are a promising new technology that has the potential to improve the effectiveness and safety of stents for the treatment of narrowed or blocked blood vessels.

The adhesion force of an electrospun nanofiber covered stent is important because it can affect the effectiveness of the stent in its intended application. A strong adhesion force can help ensure that the nanofibers remain securely attached to the stent surface, which can prevent the stent from becoming dislodged or moving out of place. This can be especially important for medical stents, where proper positioning is crucial for the successful treatment of a patient. Additionally, strong adhesion can also prevent the nanofibers from becoming detached, which can be important for applications where the nanofibers are being used to deliver drugs or other therapeutic agents. In these cases, it is important that the nanofibers remain in place and continue to release their payload over a sustained period of time. Furthermore, adhesion can also be important for mechanical stability, the stronger the adhesion, the stronger the composite material will be. Adhesion force of electrospun nanofiber covered stent plays a crucial role for the proper functioning of the stent, delivering drugs or other therapeutic agents and for mechanical stability of the material.

There is no standard method for measuring the electrospun nanofiber covered stents. In this study a method is validated for measuring electrospun nanofiber covered stents. For validating the method, initially peel tests have been done on both 2D and 3D surfaces using various adhesive tapes. Wood, steel and plastic surfaces have been used for the validation part. 2D results directly collected from the tensile testing machine while for 3D surfaces modified machine was used. The validation was completed by comparing the outcomes of 2D and 3D structures for specific surfaces in terms of increasing or decreasing forces. Here the average maximum (Fmax), average minimum (Fmin) and average adhesion force (Favg) were calculated. Later to validate the method, reproducibility was checked for 3D surfaces in the modified machine. Two persons did the adhesion test separately by following the same method for steel surfaces. From the validation part, it has been observed that the adhesion forces of 2D and 3D surfaces are quite coherent and reproducible. Similar results have been found for 2D, and 3D structured nanofiber covered stents.

After Validating the method for the modified machine, adhesion force of electrospun nanofiber covered stents was measured where stents were produced by braiding technology. The adhesion force of the electrospun nanofiber covered stents surface was evaluated in terms of different braiding structures, electrospinning set up and treatment. On average, having a higher wire density in the braiding structure exerted nearly 1.5 times higher adhesion force than having a lower wire density. Regarding the electrospinning setup, the horizontal setup showed roughly 1.5 times higher adhesion force for the electrospun nanofiber covered stent. Plasma and heat treatment were applied to the stent to improve the adhesion force between the nanofiber and stent. It was found that adhesion forces have been increased more than 2 times than untreated reference stent, while heat treatment showed more than 1.5 times increasement.

It can be noted that to get a better adhesion force, plasma treatment is a good option. Though there was a lot of variation in results observed in the modified machine for 3D cylindrical structured

adhesion force, these can be overcome by implementing different sensors and attachments in the machine.

**ACKNOWLEDGEMENTS**

I express my sincere gratitude to my thesis advisor Prof. Dr. Osman Babaarslan and Thomas Schnieders or their invaluable guidance, support, and encouragement throughout the entire research and writing process. Their expertise, patience, and understanding have been essential to the successful completion of this thesis.

**LIST OF TABLES**

**LIST OF FIGURES**

**SYMBOLS AND ABBREVIATIONS**

$A_{12}$ : Hamaker constant

BMS : Bare-metal stents

BRS : bioresorbable stents

CAD : Cardiovascular diseases

CS : Covered stents

$D_0$ : Separation distance

DES : Drug-eluting stents

F : Average load

$\gamma_1$, $\gamma_2$ : Surface energies of the two bare surfaces

$\gamma_{12}$ : Interfacial energy

ISR : In-stent restenosis

L : Length

P : Average load per unit film width

PCI : ercutaneous transluminal intervention

t : Thickness

TPU : Thermoplastic polyurethane

W : Width

$W\lambda$ : Strain-energy density

$\Theta$ : Angle

## 1. INTRODUCTION

The world health organization (WHO) reports that one of the top causes of death, cardiovascular diseases (CAD), accounted for about 32% of all fatalities worldwide in 2019. Among them, nearly 85% of the deaths happened due to stroke and heart attack. When a clot form and completely cuts off blood supply to a portion of the heart muscle, a heart attack results. A tubular medical device named a stent is used for coronary revascularization. Different types of stents are available on the market, which can be classified according to the materials, drug releases, and bio-absorbability. Furthermore, stents are also classified depending on the ailment that needs to be treated and the channel that is clogged.

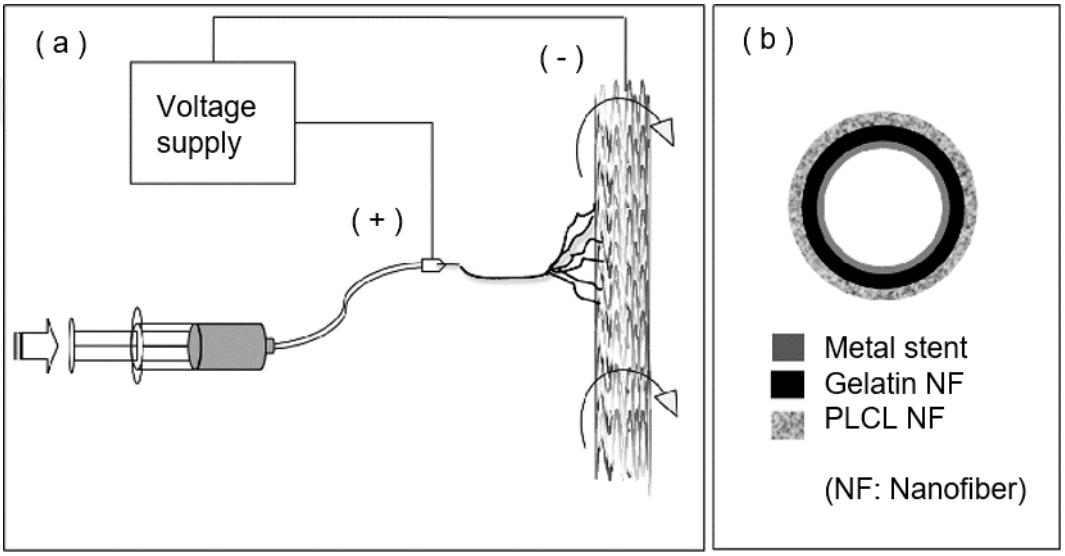


Figure.1.1. Schematic diagram of electrospun nanofiber covered stent. a) electrospinning system and b) covered stent parts (Heo et al., 2011)

Electrospun nanofiber covered stents are far more promising than other covered stents because of their thinner walls, which serve to build a physical barrier to prevent in-stent restenosis (ISR). The greater porous features of electrospun nanofiber, on the other hand, make it more biocompatible. But a higher adhesion force is required between the stents and nanofiber, where no validated method exists to measure it. This study validated a method of measuring the adhesion force using different 3D surfaces and adhesives. Where an available tensile testing machine measured the 2D structured surface's adhesion force, and a modified machine was developed for 3D cylindrical structured samples. Later on, some treatment was done to enhance the adhesion forces, which will be discussed in the next sections of this study.

## 2. PRELIMINARY WORK

### 2.1. Stents

Stents are frequently used to treat coronary artery disease (CAD). Brief descriptions of stents, their types, and the materials they are made of are provided in the following paragraphs.

#### 2.1.1. Stents and its working principle

A stent is a tubular medical device produced by different structures and implanted in the body's arteries. The development of fatty deposits called plaque causes the narrowing of the coronary artery, which is responsible for reducing blood flow, and chest pain can occur when the blood supply to the heart muscle is reduced. A heart attack occurs when a clot develops and totally stops blood flow to a part of the heart muscle. Stents are devices that assist in keeping coronary arteries open and lower the risk of a heart attack, which is the most significant advancement in percutaneous coronary revascularization. A heart attack, lung cancer, or another ailment that affects the body's airways may require the implantation of a stent. Stents that open the bile ducts, ureters, urethra, or esophagus are examples of other stents. According to the World Health Organization and the Center for Disease Control and Prevention, stents are vital for recovering from CAD, which is one of the primary causes of death worldwide and accounted for around 32% of global health in 2019. Stents were developed in the middle of the 1980s to address the issue of restenosis using percutaneous transluminal intervention (PCI). They can be divided into different types based on their expansion mechanism, coatings, treatment locations, and structure.(American Heart Association, 2017; Jamshidi et al., 2008; Schmidt & Abbott, 2018)

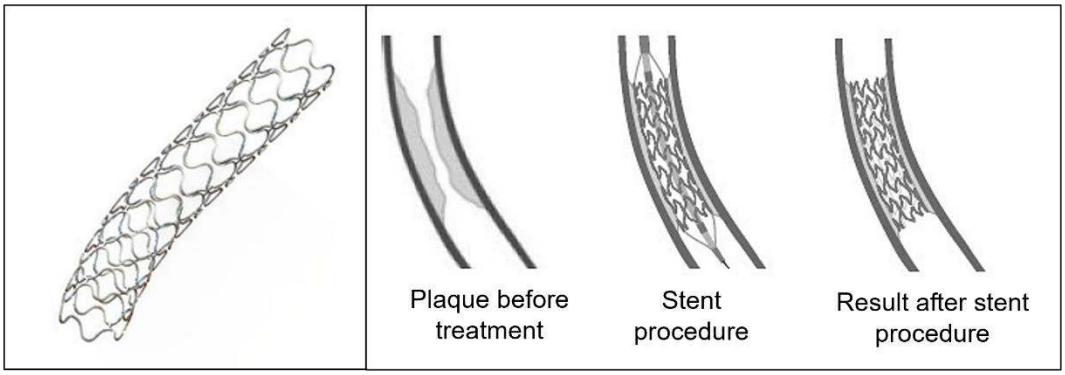


Figure 2.1: Stent and its working procedure where using stent make a path by removing plaque

#### 2.1.2. Types of stents

Many different types of stents are available, depending on the ailment that needs to be treated and the clogged channel. Table 2.1 describes the different types of stents.

Table 2.1. Different types of stents

| Stent types | Description |
|---|---|
| Coronary stents | • Known as heart stents<br>• Assist in keeping the arteries open<br>• Can be used upon doctor consultation<br>• Can be used if a person has had a heart attack or coronary artery diseases |
| Peripheral vascular stents | • Peripheral vascular stents are used in peripheral arteries<br>• Peripheral arteries can be found in the legs and arms<br>• Constructed of mesh or have a synthetic fabric covering<br>• Assist in keeping the peripheral arteries open. |
| Carotid artery stents | • Carotid artery stents can aid in treating carotid artery disease.<br>• The carotid arteries are located in the neck and are responsible for supplying blood to the brain. |
| Esophageal stents | • The esophagus is a tube that links the stomach to the throat.<br>• Esophageal stent assists in keeping the esophagus open at the time of esophageal cancer.<br>• An esophageal stent can aid with swallowing difficulties and pain, making it simpler to eat and drink. |
| Prostatic stents | • When various therapies for an enlarged prostate have failed, a prostatic stent may be required.<br>• The urethra, the tube that takes urine out of the body, narrows due to an enlarged prostate.<br>• A prostatic stent stretches to widen the urethra. |
| Ureteral stents | • Urine is transported from the kidneys to the bladder via the ureters<br>• A ureteral stent can assist in maintaining the ureter open and restoring normal urine flow.<br>• Also known as a kidney stent<br>• If a person has a kidney stone, they may require a ureteral stent. |
| Biliary stents | • The bile ducts connect the liver to the small intestine, allowing bile to pass through and aid in food digestion.<br>• Biliary stents can help persons who have a blockage in their bile duct.<br>• Metal or plastic biliary stents are commonly used. |
| Airway stents | • Airway stents keep the airways leading to and inside the lungs open.<br>• Laryngeal stents, tracheal stents, and bronchial stents are examples of airway stents.<br>• Several types of airway conditions (both malignant and benign), such as airway stenosis, benign or cancerous tumors, airway fistulas, and others, can prevent or restrict airflow and necessitate the use of an airway stent. |

Stents can also be classified into four groups according to the product's material, drug release, and bioabsorbility. They are bare-metal stents (BMS), drug-eluting stents (DES), bioresorbable stents (BRS), and covered stents (CS).

***Bare metal stents***

A stent consisting of metals like stainless steel and cobalt-chromium (CoCr) in the form of a slotted tube or coil is known as a BMS. This stent was invented in 1986 by Puel and Sigwart. This stent is utilized to achieve a higher level of strength and stretchability than others. The elimination of constructive remodeling and elastic vessel wall recoil is its advantage. Metals used to make metal stents have low biocompatibility with the human body, making blood clots more likely. Endarterectomy and thrombus formation after the procedure produce several side effects, such as acute vascular blockage and persistent complications, such as restenosis, resulting from these issues. Approximately 30% of patients have neo-intimal hyperplasia or in-stent restenosis.(Mittal et al., 2014)

***Drug-eluting Stents***

The introduction of drug-eluting stents, which have lowered the ISR rate from 10–40% to 10 %, was a milestone in stenting technology. A drug-eluting stent comprises three main parts: the drug, the polymer coating, and the stent itself. Non-degradable or degradable polymers carrying an immunosuppressant or anticancer medication are placed on the surface of metal stents. Thin strut stents promote early reendothelialization, which is a benefit of DES. Mechanical stability over a long period of time is also an advantage of DES, but as DES differs from human tissue, there is a chance that the stents will be rejected when implanted in the human body. The rate at which the drug is released is determined by the molecular weight of the polymer and the properties of the drug included within. Blood compatibility, tissue compatibility, non-toxicity, and stability are all requirements for materials covered on the stents' surface. For the interventional treatment of coronary artery disease, drug-eluting metal stents are now the gold standard. While drug-eluting metal stents inhibit neointimal hyperplasia, they have a number of drawbacks, including the risk of late and very late stent thrombosis, vascular vasomotion restriction, and a chronic local inflammatory reaction due to the permanent implantation of a metallic cage, which is recognized as a foreign body by the body. (Lee et al., 2018; Mitsuo et al., 2015)

***Bioresorbable Stents***

BRS was introduced as a promising solution that was created to overcome the limitations and problems associated with DES, such as late ISR and permanently caging the vessel. The idea behind a BRS is to maintain the vessel temporarily before it is degraded and reabsorbed by the body,

aiding in vascular repair and regaining vasomotion. Not only biodegradable polymers like poly-L-lactic acids and their copolymers but also metals like magnesium alloys, iron-based alloys, and pure zinc are now being investigated as materials for BRS, with some of them undergoing clinical trials. Lack of radial strength is the limitation of BRS.(Ang et al., 2018)

***Covered Stents***

A covered stent is one that has a material covering its length and circumference. As a result, following implantation, a covered stent might create a physical barrier between the vessel wall and the blood. A number of materials can be used to cover stents. Metallic stent platforms with a synthetic or biological membrane were first designed to solve stenting's shortcomings, including thrombosis and restenosis, by separating thrombogenic struts from the bloodstream and limiting smooth muscle cell migration, which causes neointimal hyperplasia. Covered stents are a viable alternative to surgery for the exclusion of coronary aneurysms and may have a function in the treatment of friable embolization-prone plaques.(Kilic et al., 2016)

There are several problems that arise with the covered stents, but a new covered stents design with;

- reduced thickness and better membrane material
- lower deployment pressure, and medication inclusion
- increase saphenous vein grafts (SVG) intervention performance. There are several problems that arise with the covered stents, but a new covered stent design with reduced thickness, better membrane material, lower deployment pressure, and medication inclusion increases saphenous vein graft (SVG) intervention performance.

Figure 2.2: Nanofiber covered over metal stent for coronary artery disease

**2.1.3. Electrospun nanofiber covered stents**

Among different stent types, nanofiber-covered stents are one of them, where nanofiber is covered by the electrospinning method on BMS. Different polymers are enclosed within the stent's

length and circumference. The nanofiber-covered stents will address many of the limitations of the currently covered stents. In comparison to other covered stents, the nanofiber covered stents (NCS) could potentially aid in lowering the wall thickness by introducing a two-layer low-profile design (bare metal stents + nanofibrous membrane) as acute thrombosis, delayed/incomplete reendothelialization, and restenosis was all reported in patients who used other covered stents having high wall thickness. NCS creates a physical barrier to prevent ISR where the nanofiber cover is not only biocompatible but also biodegradable. (J. Guerra & Ciurana, 2009; M. C. Petrie et al., 2006)

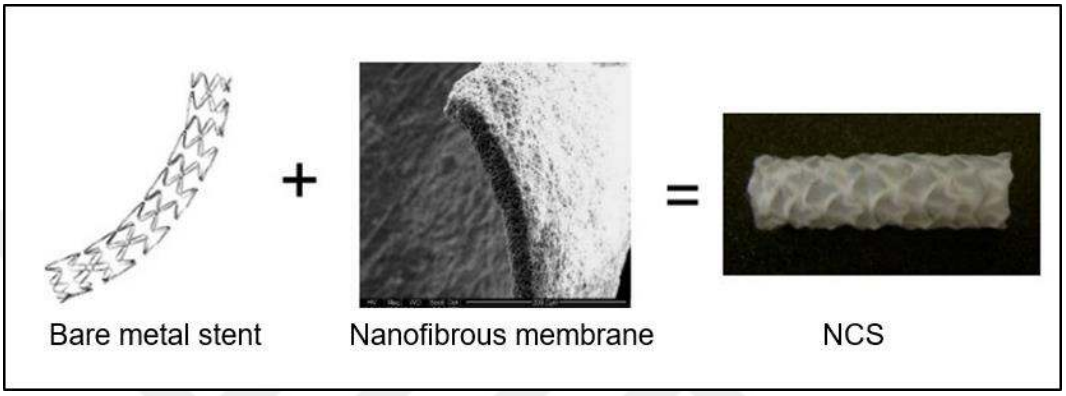


Figure 2.3: Electrospun nanofiber covered stent (J. Guerra & Ciurana, 2009)

### 2.1.4. Stents materials

In the previous few decades, stent materials have been thoroughly researched. The materials used in stents have swiftly changed and diversified since the introduction of the first stainless-steel devices. The main research lines have been to understand how manufacturing processes affect material properties, develop novel materials, and analyze new coatings and their effects on biological aspects. Table 2.2 summarizes the most common materials now in use or under development.

Table 2.2. Materials used in stents (J. Guerra & Ciurana, 2019)

| Type | Material | Description |
|---|---|---|
| Nondegradable | Nitinol (NiTi) | • Nitinol is a nickel-titanium metal alloy<br>• Shape memory (SME) and superelasticity (SE) are two key features<br>• Ideal for self-expandable stents. |
| | 316 stainless steel (SS316) | • Known as marine-grade stainless steel<br>• Chromium, nickel, and molybdenum alloy of steel<br>• Have good strength and corrosion resistance<br>• Popular choices for biomedical implants like stents |
| Fully degradable | Magnesium (Mg) | • Magnesium ranks third in terms of structural metal usage<br>• Magnesium is employed in materials and alloys<br>• Super strong and lightweight. |

| | | |
|---|---|---|
| | | • Utilized due to magnesium's proclivity for corroding, creeping at high temperatures, and combusting |
| | Polycaprolactone (PCL) | • Biodegradable polyester<br>• Have a low melting point (60°C) and a glass transition temperature of around 60°C<br>• Degradation is caused by hydrolysis of its ester bonds |
| | Poly-l-lactide acid (PLLA) | • Biodegradable aliphatic thermoplastic polyester<br>• Made from renewable materials like maize starch<br>• Degradation is caused by hydrolysis of the ester bonds |
| | Iron | • potential for bioabsorbable metals<br>• Has low toxicity and low corrosion resistance in biological environments<br>• No clinical study has yet been published |
| | Zinc | • Have optimal degradation rate for bioabsorbable coronary stents<br>• Degradation rate is lower than magnesium alloys but greater than pure iron |

**Metal stents properties**

The stents struts are the device's backbone, and their composition determines several of its features, including radial strength, deliverability, and restenosis risk. Table 2.3 demonstrates the clinical impact of the properties of the physical stent.

Table 2.3. Clinical impact of physical stents characteristics (Schmidt & Abbott, 2018)

| Physical component | Clinical correlation |
|---|---|
| Choice of metal→strut thickness | Restenosis, inflammation, radial strength, radio-opacity |
| Cell size and design | Plaque prolapse, side branch access, gaps in drug delivery |
| Connectors | Flexibility and deliverability, longitudinal strength |

Stent materials properties are,

- To avoid generating an immunological reaction, the metal used must be biocompatible, corrosion-resistant, and radio-opaque.
- Inflammation and subsequent restenosis are caused by hypersensitivity to the metal in the stents; therefore, finding a biologically inert metal is critical for the device's safety and efficacy.
- Elastic modulus refers to a material's rigidity, and a material with a high elastic modulus is suitable for stent fabrication. Because nickel-titanium alloy nitinol has a low elastic modulus, it deforms quickly when subjected to opposing forces along an axis.

- A material's yield strength is its capacity to resist plastic deformation. Unless they are subjected to a force greater than their yield strength, materials with high yield strength will keep their original structure.
- During a cardiac cycle, coronary stents are subjected to different forces and must be able to sustain these forces without yielding over time. That is why high tensile strength is required.

### 2.1.5. Stents manufacturing process design

The obstacles to using a stent, whether a BMS, DES, BRS, or ETS, are quite similar. Initially, mechanical properties need to be the focus while the manufacturing process and additional properties are followed, respectively. Figure 2.4 depicts the pyramid of the stent manufacturing process design. It represents the most important factors to consider while designing and manufacturing this medical device. Table 2.4 illustrates the variables depending on this process design.

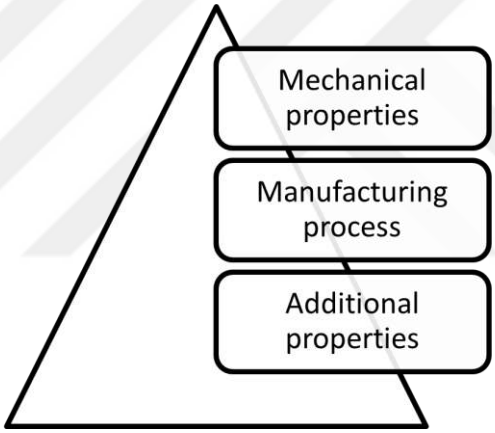


Figure 2.4. Pyramid of stents manufacturing process design (J. Guerra & Ciurana, 2019)

Table 2.4. Process designs variables(J. Guerra & Ciurana, 2019)

| Process design factor | Variable |
|---|---|
| Mechanical properties | material, geometry, application |
| Manufacturing process | material, stents type |
| Additional properties | stents type, application |

## 2.2. Adhesion

### 2.2.1. The Basic Concept of Adhesion

The term adhesion is used to describe a common phenomenon or situation in which two bodies are stuck together. Adhesion is defined as "the state in which two surfaces are held together by interfacial forces, which may consist of valence forces, interlocking forces, or both," according to ASTM D 907. Figure 2.5 represents the adhesion and cohesion forces.

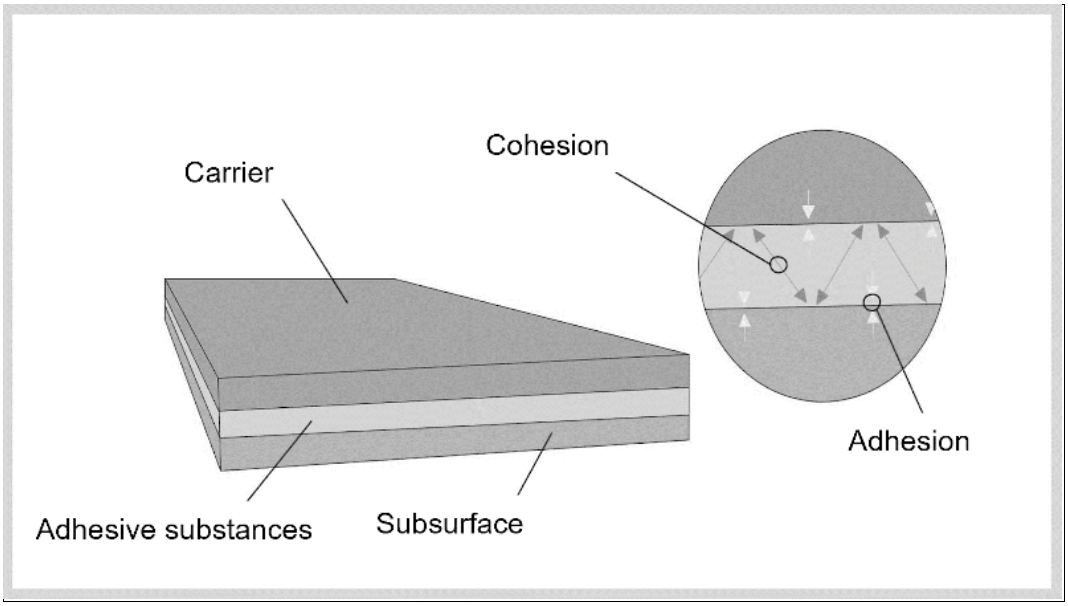

Figure 2.5. Adhesion and cohesion

### 2.2.2. Magnitude of adhesion

Adhesion refers to both the basic atomic and molecular forces that hold the two phases together, as well as the results of destructive adhesion tests, such as peel strength. The widespread understanding of the relationship between fundamental and practical adhesion has advanced significantly in recent decades. "Fundamental" adhesion is a term that describes the forces that exist between atoms at the interface. It is also referred to as true adhesion. For fundamental adhesion, naturally, the concept is bound to one of the adhesion theories and a specific model for the interface in question. It can be described in terms of energies or forces.

On the other hand, practical adhesion is the destructive test of adhesion that is also said to measure the adhesion of a joint or coating. The term "adhesion" here refers to the number obtained from shear, tensile, and another testing. It could be a characteristic related to peel strength or fracture mechanics.(Packham, 2005; E. M. Petrie, 2007)

The idea of integrating diverse materials into a single film structure is based on the assumption that the layers will stick together. The layers will delaminate if there is insufficient adhesion, and the function will be compromised. Good interlayer adhesion is required for the film's tensile strength, stiffness, and other physical qualities. The fabrication method, the chemistry of the layers, and the relative arrangement of the layers to each other all influence adhesion. If the multilayer film is created from prefabricated films or substrates, an adhesive or glue will be needed to join them together and contact time, temperature and quench conditions play vital roles in adhesion.(Morris, 2017)

### 2.2.3. Adhesives tapes

Adhesive tape is a material that has adhesive film and is used to connect or join objects together instead of utilizing fasteners, screws, or welding. Adhesive-coated backing or carrier material of adhesive tapes can be made out of paper, plastic film, fabric, foam, felt, non-woven, PET, polyimide, PVC, rubber, silicone, acrylic film, filament, foil, and other materials made of paper, plastic film, fabric, foam, or foil. The physio-chemical interaction between the adhesive material and the surface to which it is applied significantly impacts adhesion. Adhesives can firmly and permanently adhere at least two surfaces together. A schematic view of adhesive tape has been illustrated in Figure 2.6

Adhesives are chosen for their ability to hold and adhere, and they are often made of materials with strong shear and tensile strength. Several factors influence the selection of adhesives to get a good or desired adhesion. Table 2.5 shows the factors influencing adhesive selection. Adhesives come in a variety of forms, including acrylic, epoxy resins, rubber-based, silicon, polyurethane, and isocyanate and can be classified in different ways. Table 2.6 demonstrates the classification of adhesives.(Packham, 2005; E. M. Petrie, 2007)

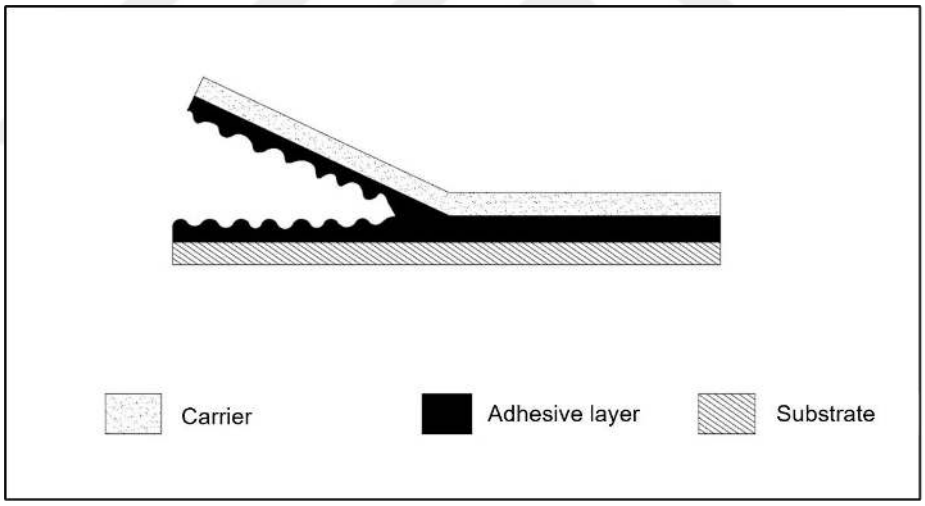


Figure 2.6. Schematic view of adhesive tape

Table 2.5. Factors influencing adhesive selection (E. M. Petrie, 2007)

| Factors | Parameters |
|---|---|
| **Stress** | Tension, shear, peel, cleavage, fatigue |
| **Chemical** | External, internal |
| **Exposure** | Weathering, light, oxidation, moisture, salt spray |
| **Biological** | Bacteria or mold, rodents or vermin |
| **Temperature** | High, low |
| **Working properties** | Applications, bonding range, blocking, curing rate, storage stability, coverage |

Table 2.6. Classification of adhesives (Packham, 2005; E. M. Petrie, 2007)

| Classified method | |
|---|---|
| **Origin** | 1. Natural<br>2. Synthetic |
| **Bonding temperature** | 1. Cold setting<br>2. Room temperature setting<br>3. Intermediate temperature setting<br>4. Hot setting |
| **Method of bonding** | 1. Pressure sensitive<br>2. Hot melt<br>3. Chemical settings<br>4. Solvent release |
| **Function** | 1. Structural<br>2. Non-structural |
| **Chemical composition** | 1. Thermosetting<br>2. Thermoplastics<br>3. Elastomer<br>4. Hybrid |
| **Form** | 1. Liquid<br>2. Paste<br>3. Powder<br>4. Mastic<br>5. Film<br>6. Other |

### 2.2.4. Work of adhesion

The work of adhesion is used to characterize the propensity of polymer adherence via the idea of surface energy from a conventional thermodynamic perspective. As from the equation below, the work of adhesion, W, is defined as the energy change per unit area caused by the development of a new interface and the elimination of two bare surfaces. The adhesion work is distinguished between two states: contact and separation.

$$W = \gamma 1 + \gamma 2 - \gamma 12 \quad (2.1)$$

Where; $\gamma_1$ and $\gamma_2$ are the surface energies of the two bare surfaces, $\gamma_{12}$ is the interfacial energy. If the surface is the same materials, which means: $\gamma_1 = \gamma_2$, and $\gamma_{12}=0$ , then W is called the work of cohesion.

Intermolecular attractive interactions dominate the work of adhesion when two smooth polymer surfaces come into close contact within a few nanometers. The primary intermolecular interaction is the van der Waals dispersive force. Polar contacts, hydrogen bonding, acid-base interactions, and others are examples of intermolecular interactions. The work of adhesion could be computed from the van der Waals forces if other types of intermolecular interactions could be ignored.

$$W = A12/\ 12\pi D02 \quad (2.2)$$

Where; $A_{12}$ is the Hamaker constant, which only depends on the surface chemistry of the materials. $D_0$ is the separation distance.

### 2.2.5. Importance of adhesion in implants

The coating-substrate adhesion is the most critical quality among all the mechanical qualities that regulate the performance and functionality of any coated biomedical implant, especially for load-bearing implants, regardless of the exact coating process used. In order to provide any practical benefit, the coating must be properly attached to the substrate. Failure of the coating to adhere to the substrate or delamination of the coating from the substrate results in poor implantation and insecure long-term performance. De-adhesion is the separation of the coating from the substrate due to mechanical or thermal stress, corrosion, or chemical deterioration through cracking, delamination, spallation, chipping, or plastic deformation. As a result, adhesion assessment is vital for implantable biomedical devices to achieve the desired functionality and endurance.

### 2.2.6. Methods of adhesion measurement

The adhesion property of bulk materials can be investigated in various ways. Researchers have regularly addressed adhesion testing procedures. Research into adhesion measuring techniques began in the 1950s and has resulted in the creation of a wide range of adhesion measurement techniques. Mittal published a list of approximately 300 adhesion measurement techniques in 1995. There are three types of adhesion measurement methodologies for films and coatings: qualitative, semi-quantitative, and quantitative methods. There are a lot of mechanical test methods for adhesion measurement, such as (Lei et al., 2016)

- Cross-cut test
- Peel test
- Scratch test
- Pull-off (tensile) test
- Single-lap shear test
- Blister test
- Micro & nanoindentation test
- Small-punch test
- Micro & nanoscale tensile testing
- Four-point bending test
- Others

### 2.2.7. Peel test

Peeling is a method for determining how well flexible and rigid substrates adhere to one another. A flexible substrate is torn away from a stiff substrate at a certain speed in a peel test which is constant over the test, and the result is found as a peeling force. The peeling force determines the degree of adhesion between stiff and flexible substrates. As demonstrated in Figure 2.7 multiple peeling procedures are routinely utilized to separate the flexible substrate from the rigid substrate. The flexible substrate is typically peeled at a predetermined angle in a flexible-rigid substrate system; however, when both materials joined are flexible, such as laminated plastic films, a T-peel test can be performed. The climbing drum peel test is an option for relatively rigid materials. The results of all peel tests are plotted as a function of peel force and way. Peel tests are commonly conducted at peel angles of 90 or 180 degrees or in a T-peel configuration, depending on the practical considerations of the adhesive bond. When peeled at a steady velocity, the peel strength is defined as the amount of force acting on the width of the bonding surface. The peel force remains constant at the start of the test, but as the test progresses, it tends to fluctuate to an average value. Separation at either interface or inside one of the two-component layers can cause failure if the layer breaks apart instead of detaching. The amount of peel force accurately represents the work of detachment or cohesive fracture. (McMullin, 2016)

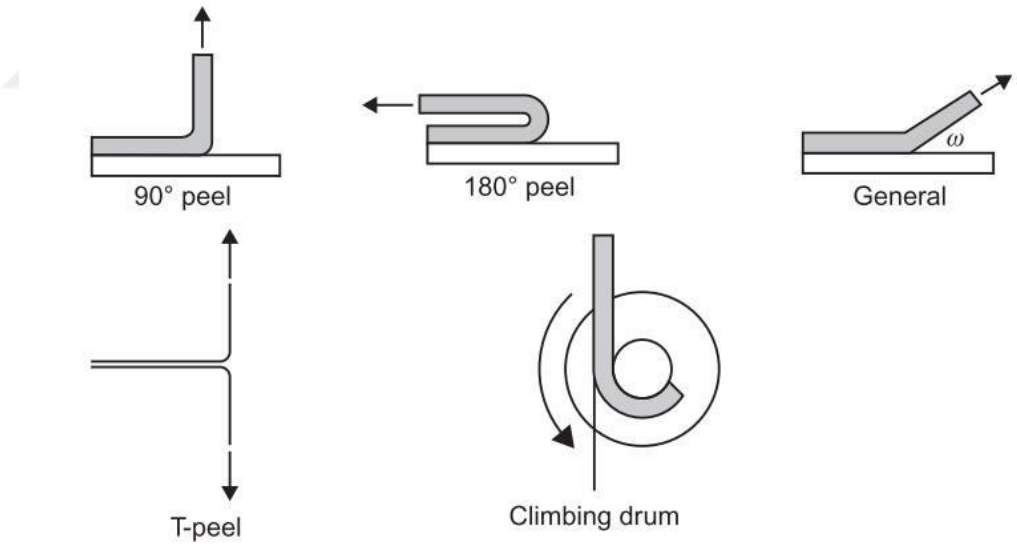


Figure 2.7. Different configurations for peeling test (McMullin, 2016)

In the peel test, a coating of a specific width (w) and thickness (t) is peeled for a specific distance (L) from the substrate at a given angle (θ) by holding onto the coating directly or with some backing material bonded to it, as shown schematically in Figure 2.8. The nominal adhesion strength is calculated using the average load at stable peel propagation, F, which corresponds to the plateau on the recorded load-displacement curve, or the average load per unit film width,

$$P = F/W \tag{2.3}$$

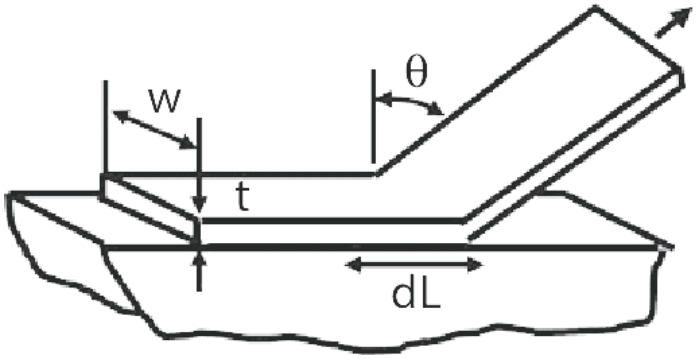


Figure 2.8. Schematic of peel test (Lei et al., 2016)

### 2.2.8. Factors affecting peel energy

***The thickness of the adhesive layers***

The highest tensile stress that can be generated in a linearly elastic glue is projected to be inversely related to the square root of the adhesive layer thickness. It has been misinterpreted that the peel force is proportional to the adhesive thickness. Peel force becomes independent of thickness for reasonably large thicknesses. As the thickness of the sticky layer rises, the peel force increases due to energy dissipation inside the bulk of the glue, as seen in Figure 2.9. When compared to the overall thickness of the adhesive layer, the highly stressed region surrounding the line of detachment is now minimal, and the principal dissipation process no longer involves the entire layer of adhesive.

In general, the peel force increases in proportion to the thickness of the peeling layer. This is due to the energy lost when the layer was bent away from the interface. The bending stresses in a thick peeling strip are low, and the strip remains relatively elastic while peeling progress. As a result, just a small amount of energy is dissipated within it. However, if the strip is thin enough, the bending forces may be sufficient to cause plastic deformation. (McMullin, 2016)

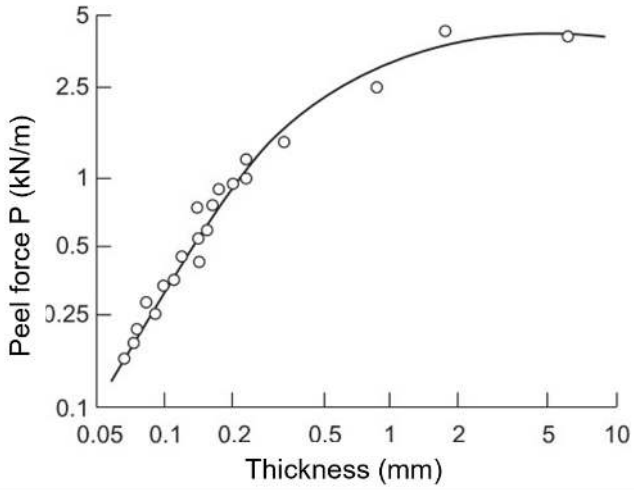


Figure 2.9. Dependence of peel force upon adhesive layer thickness for an elastomer detaching from a polyester substrate (McMullin, 2016)

***Peel angle***

The following equation can demonstrate peel energy,

$$P = F/b\ (\lambda - \cos\omega) - W\lambda \qquad (2.4)$$

Where P is peel energy, F is applied force, b is distance, strain-energy density $W\lambda$ for the extension to $\lambda$ and t for thickness.

As the peel angle changes, bending losses change, and the balance between shear and cleavage forces at the peel front changes, altering energy losses at the peel front: all of these factors could have a considerable impact on P, causing deviations from the angle dependence anticipated by equation. (Packham, 2005)

***Rate and temperature***

As demonstrated in Figure 2.10, the rate of peel and temperature have a direct impact on the peel strength of pressure-sensitive adhesives made up of soft elastomeric blocks. Peel force increases with the rate generally, especially at lower rates, and failure occurs wholly within the adhesive layer, which fails by flowing apart. An abrupt switch to interfacial separation occurs at a critical peel rate at much lower peel pressures. The molecular weight of the polymeric adhesive and its segmental mobility is directly impacted by the rate and temperature during this transition.

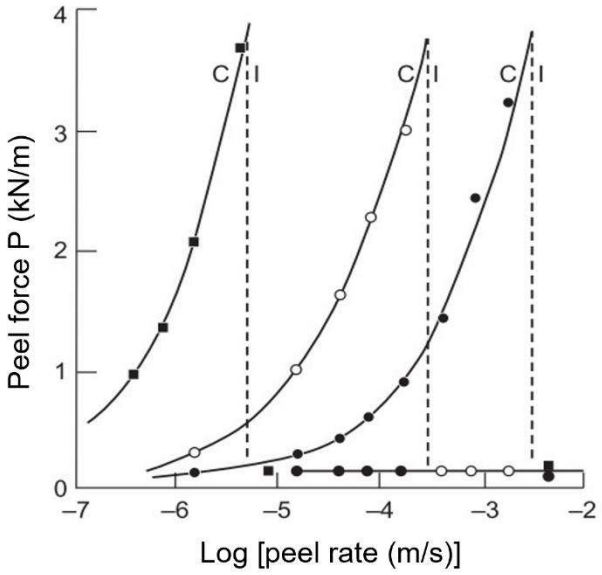


Figure 2.10. Relation between peel rate and peel force (McMullin, 2016)

### 2.2.8. Advantages and disadvantages of peel test

Peel tests provide two advantages over other similar test methods. First, failure proceeds at a controlled rate and secondly, the peel force is a function of the work of detachment or the work of cohesive fracture. The amount of energy required to detach a unit area of interface and the amount of energy consumed per unit area of material ripped will be determined by the work of detachment or work of cohesive fracture values.

Even though the peel test has a simple test geometry for determining bond breakage strength, it has significant flaws. Several investigations have proven that the peel test is a reliable assessment method only in particular circumstances.

## 2.3. Electrospinning process

Electrospinning is one of the most popular methods among researchers over the last decade for electrostatic fiber production due to its versatility and prospective applications in a wide range of fields such as filtration, nano catalysis, biomedical, health care, pharmaceutical, wound dressings, environmental engineering, protective clothing, enzyme immobilization and so on. It has been controlled over fiber dimension and controllable pore structure to produce different micro/nanofibrous fabrication and structures such as tubular structures, aligned nanofibers, core-shell nanofibers, nanofibrous yarn, and nanofibrous structures with different 2D or 3D shapes. In electrospinning, electrical forces are used to produce polymer fibers from polymer solutions of both synthetic and natural polymers with diameters ranging from 2 nm to several micrometers. (Bhardwaj & Kundu, 2010; Xue et al., 2017)

The name electrospinning is derived from electrostatic spinning and was first used in 1994, but its origins can be traced back more than 60 years. Formhals published a series of patents from 1934 to 1944 that described an experimental setup for producing polymer filaments using an electric field. More than 200 universities and research institutes are working on various aspects of the electrospinning process, which indicates its popularity. Electrospun nanofibers have several advantages, such as ease of manufacturing, biomimetic structure, high surface area to volume ratio, flexibility, and controllability of nanofiber composition. However, there are a few challenges that limit the application of electrospinning. Bottleneck in throughput at the production time for lack of cellular migration along with non-uniform cellular distribution in tissue engineering. (Huang et al., 2003; Liang et al., 2007; Ramakrishna S et al., 2006; Yarin & Zussman, 2004)

A schematic diagram of the electrospinning process is shown in Figure 2.11. For the typical electrospinning setup, there are three major components, and they are the collector, spinneret, and high voltage power supply. The setup can be horizontal or vertical, along with different types of collectors such as plates, metal screens or rotating mandrels. Before introducing the process, most of the polymers need to dissolve in solvents and then introduce the polymer in a capillary tube for electrospinning. Room temperature with atmospheric conditions is necessary to conduct the electrospinning process, and it is necessary to conduct it within a chamber for climatations and safety cause some of the polymers emit harmful or unpleasant smells. According to the applications and characteristics, natural and synthetic polymers are used for electrospinning. Silk fibroin, collagen, gelatin, chitosan, cellulose acetate, and casein are used among the natural polymer.(Kidoaki et al., 2005; Liang et al., 2007; Zeugolis et al., 2008)

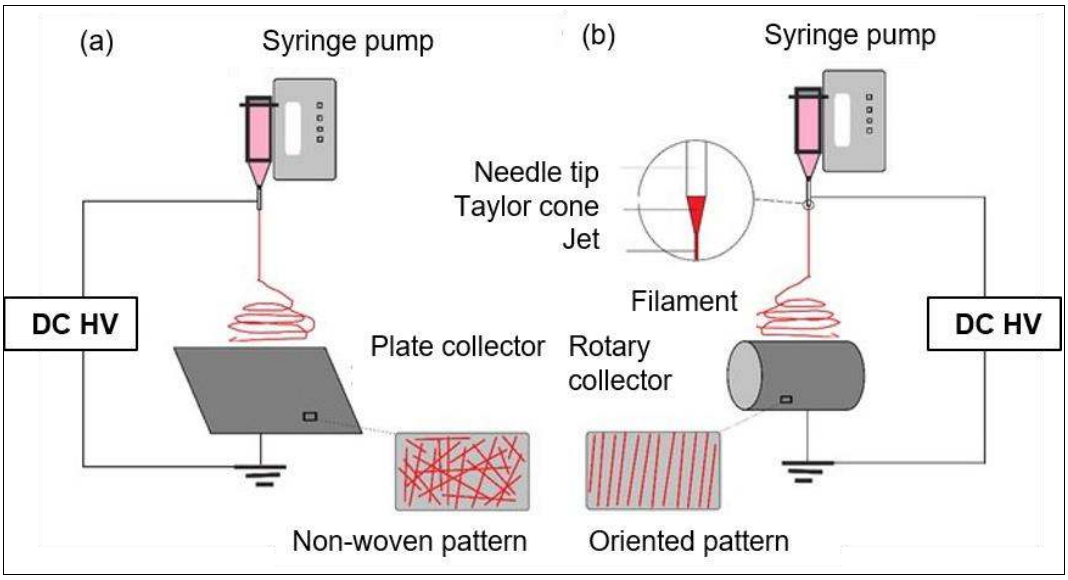

Figure 2.11. Schematic view of the electrospinning process (Esfahani et al., 2017)

Several factors or parameters influence the electrospinning process and can be classified into solution, ambient, and process parameters. Table 2.7 shows the parameters, including its class. Every parameter has an effect on fiber morphology. (Bhardwaj & Kundu, 2010; Chong et al., 2007; Li & Xia, 2004)

Table 2.7. Parameter of the electrospinning process

| **Solution parameter** | **Ambient parameter** | **Process parameter** |
|---|---|---|
| Viscosity | Humidity | Applied voltage |
| Conductivity | Temperature | Feed rate/flow rate |
| Molecular weight | | Types of collector |
| Surface tension | | Tip to collector distance |
| Concentration | | |

For having successful electrospinning process, it is required to have appropriate solvent is cause dissolving the polymer into a suitable solvent is the first step of the process. Solvents should have certain characteristics, such as low volatility, high vapor pressure, and a high boiling point, as well as the ability to retain the polymer solution's integrity. As the electrospun nanofiber's morphology and size affect surface tension and different solvents contribute to different surface tension, it is necessary to select suitable solvents. Moreover, lower surface tension is not appropriate for the electrospinning process. Chloroform, Dimethyl formamide, Hexafluoro isopropanol, Tetrahydrofuran Trifluoro ethanol, Acetone, Water, Methanol, Acetic acid, Formic acid, Dichloro methane, Ethanol, Tri fluoro acetic acid are commonly used solvents in electrospinning process. (Bhardwaj & Kundu, 2010; Fong & Reneker, 1999)

## 3. MATERIAL AND METHOD

Figure 3.1 shows the systematic approach of this study. Having problems in measuring the adhesion force of the electrospun nanofiber covered stent influenced to valid method with the modified machine. Then validated method is used to measure the adhesion force of the electrospun nanofiber stent. Different treatments were applied after observing adhesion failure on stents in order to increase adhesive force.

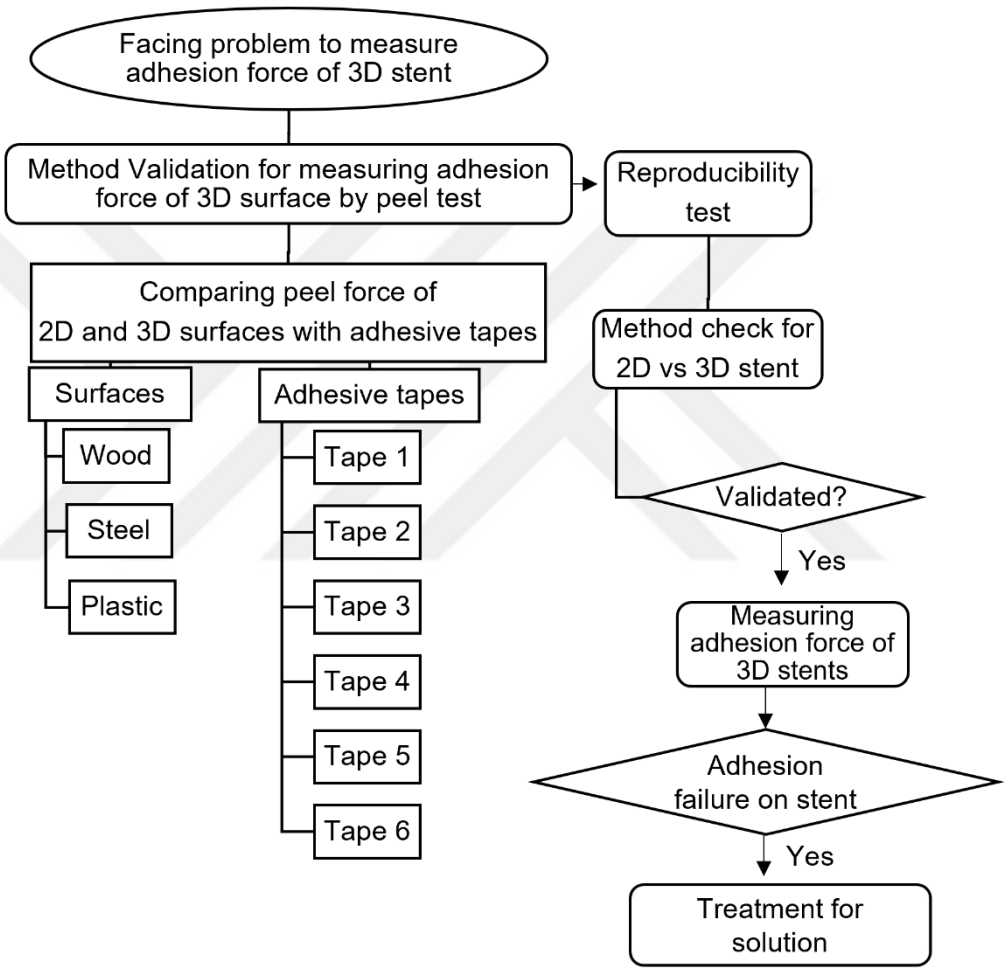


Figure 3.1. Flowchart for an overview of the systematic procedure for method validation of 3D stent adhesion force measurement and solution for the treatment

### 3.1. Materials

In this study, a method was validated initially to measure the adhesion force between a coating and a 3D cylindrical structure. For this, various surfaces and adhesive tapes are applied to 2D and 3D cylindrical structures. Table 3.1 represents the materials that are used for the method validation part. Here, for 2D surfaces, the length and width were 20 cm and 3 cm, whereas, for the 3D cylindrical surfaces, the length was 5 cm with 3 cm diameter, shown in Figure 3.2

Table 3.1. Materials used for the methods validation part

| Surfaces | Tape (adhesive) |
|---|---|
| Steel | Tape 1 (Natural Rubber) |
| Wood | Tape 2 (Water-dissolved acrylate green) |
| Plastic | Tape 3 (Synthetic rubber) |
| | Tape 4 (Self-adhesive) |
| | Tape 5 (Hotmelt) |
| | Tape 6 (Water-based acrylate) |

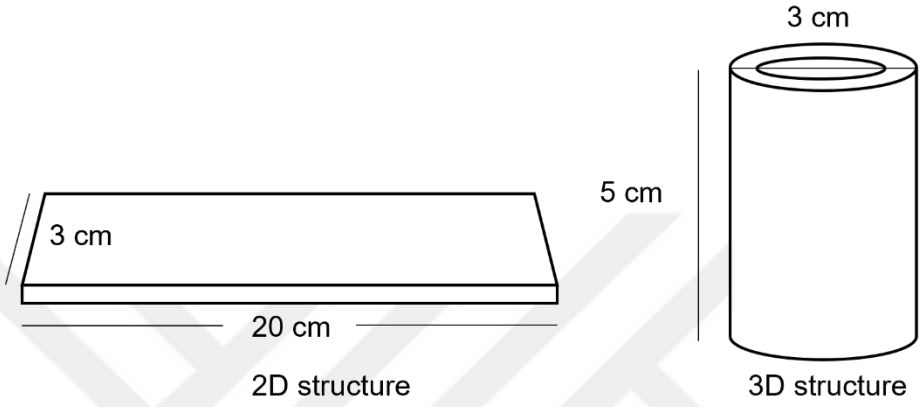


Figure 3.2. Schematic view of the 2D and 3D surface

For producing stents, nitinol wire is used, which is covered with TPU nanofiber by an electrospinning process. TPU is used by Lubrizol Corporation, Wickliffe, Ohio, United States.

## 3.2. Methods and experimental

### 3.2.1. Validation

Peel tests on both 2D and 3D surfaces using various adhesive tapes have been conducted to validate the modified machine adhesion force approach. The method has then been validated by analysis of the outcomes. The average maximum, average minimum, and overall average force have all been computed for the outcome analysis. 2D results were directly collected from the tensile testing machine, and 3D part results were collected from the modified machine. To have a uniform result for the 3D part, results from 25 mm to 60 mm were only counted. As every test has been done five times, the average maximum (Fmax), average minimum (Fmin) and average adhesion force (Favg) were calculated by taking the result for each test and averaging them. The standard deviation has also been determined. The validation was completed by comparing the outcomes of 2D and 3D structures for specific surfaces in terms of increasing or decreasing forces. Later, two users independently tested the adhesion force for a specific surface and an adhesive tape with a customized machine to ensure reproducibility.

### 3.2.2. 2D peel test

2D peel test is done by following DIN ISO 8510-2. For this tensile testing machine has been used. For the preparation of the samples, initially, 2D surfaces were cleaned according to ISO 17212 and then the samples were conditioned according to ISO 291 after that peel test. Figure 3.3 depicts the Flowchart of sample preparation. A pressure roller was used to give pressure on the surfaces two times without extra pressure to ensure uniform attachment of the adhesives. The weight of the pressure roller was 380 gm, and it was used by hand. For each surface, 6 types of adhesive tape have been used, so 18 different combinations. Five specimens have been tested for each combination. Table 3.1 shows the used tapes and 2D samples before the peel test measurement using a tensile testing machine. A schematic view of tensile testing machines is illustrated in Figure 3.4. Here, the test speed was 50 mm/min for these tests, and the load was 200N.


Figure 3.3. Flowchart of sample preparation for 2D samples

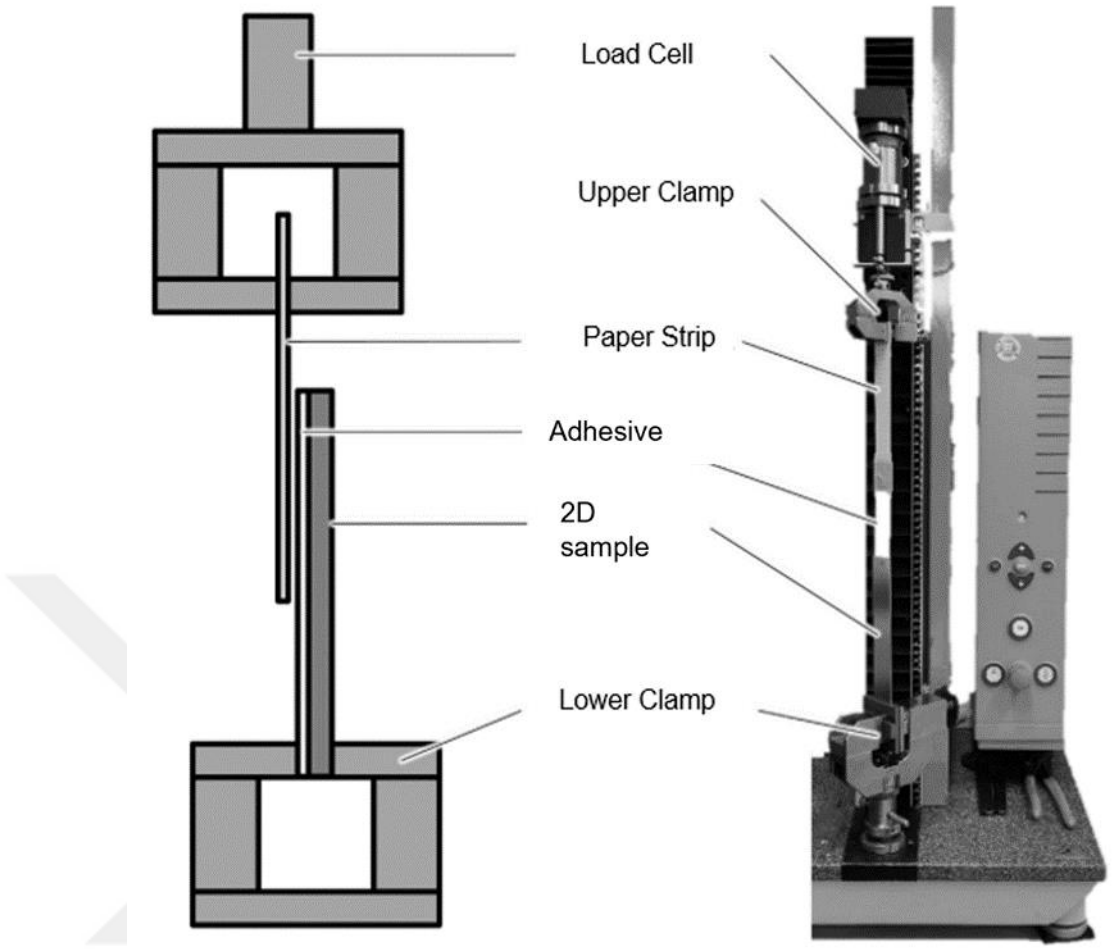


Figure 3.4. Left: schematic structure of the tensile testing system and right tensile test system for 2D sample

### 3.2.3. 3D sample peel test

For the 3D samples test, a modified machine has been developed. Figure 3.5 illustrates the machine setup for the 3D cylindrical structured peel test measurement with a close view. For attaching the 3D sample, a setup with a movable mandrel was fixed to the lower part of the machine. As shown in the figure, a load cell was attached to the machine's upper part, which was movable in a longitudinal direction. A flexible clamp was also attached to the load cell to clamp the adhesive part. For the peel test, DIN ISO 8510-2 has been followed, similar to the 2D sample test. Surface preparation and conditioning for 3D samples were performed similarly to 2D samples. Here the peel angle was kept at almost 90 degrees. The test speed was also 50 mm/min. 3 mm of the adhesive part was grabbed by the clamp. The peeling test has been done following similar steps in Figure 3.3. At the time of running, the load cell goes upward by holding the adhesive part, and the 3D surface rotates due to adhesive upholding. Forces were stored in the position of displacement. Table 3.2 shows the parameter for the test.

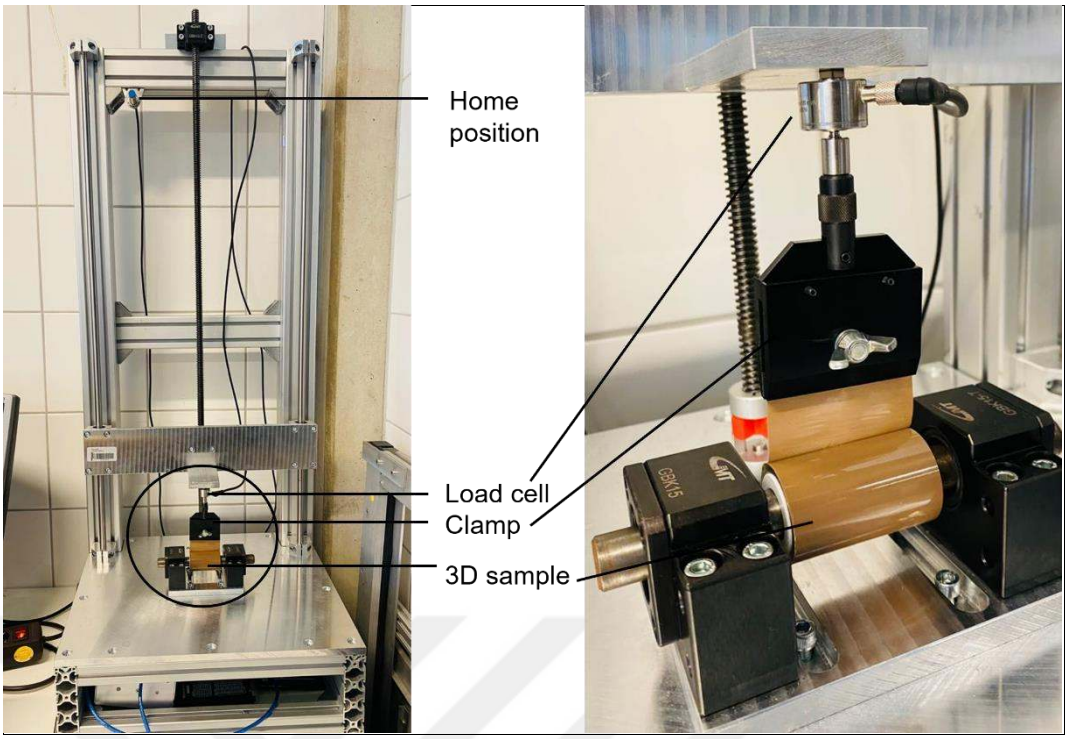

Figure 3.5. Modified machine set up with close view for 3D cylindrical sample's peel test

Table 3.2. Parameter for the 3D peel test

| Parameter | Value |
|---|---|
| Peel Angle | 90 degrees |
| Peeling speed | 50 mm/min |
| Grabbing part | 3 mm |
| Calculated length | 25 – 60 mm |

### 3.2.4. Braiding of stent

For stent manufacturing, nitinol wire is used to produce stents by a 3D steeger braiding machine, which is represented in Figure 3.6. First, nitinol wire was wound in 24 small spools by a rewinding machine. Then the spools were placed in the braiding machine. Here the circular speed of the braiding machine was kept at 20 rpm, and the forwarding machine was kept at 2 and 5 picks/cm (pix/cm). The produced stent's angle was 45°, and the mandrel diameter was 3 cm. Additionally, another braided structure was produced with a 1 cm mandrel diameter for having the 2D structure of the stent. Figure 3.7 shows the outer and inner view of the braided stent. For 2D structures, 3D braided stents are cut lengthwise, and the outer edge is taped to maintain their shape. Then 2D stents were placed between two flat steel plates and locked it. Then the 3D and 2D structures were heated at $600^0$ C for 20 minutes to gain shape memory and stabilize their shape.

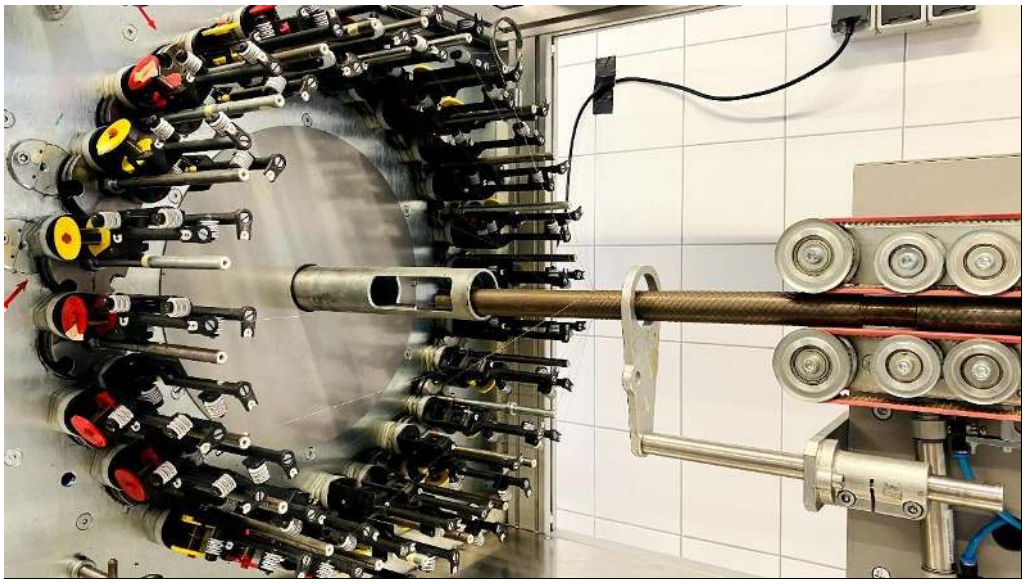

Figure 3.6. Steeger braiding machine for producing stents

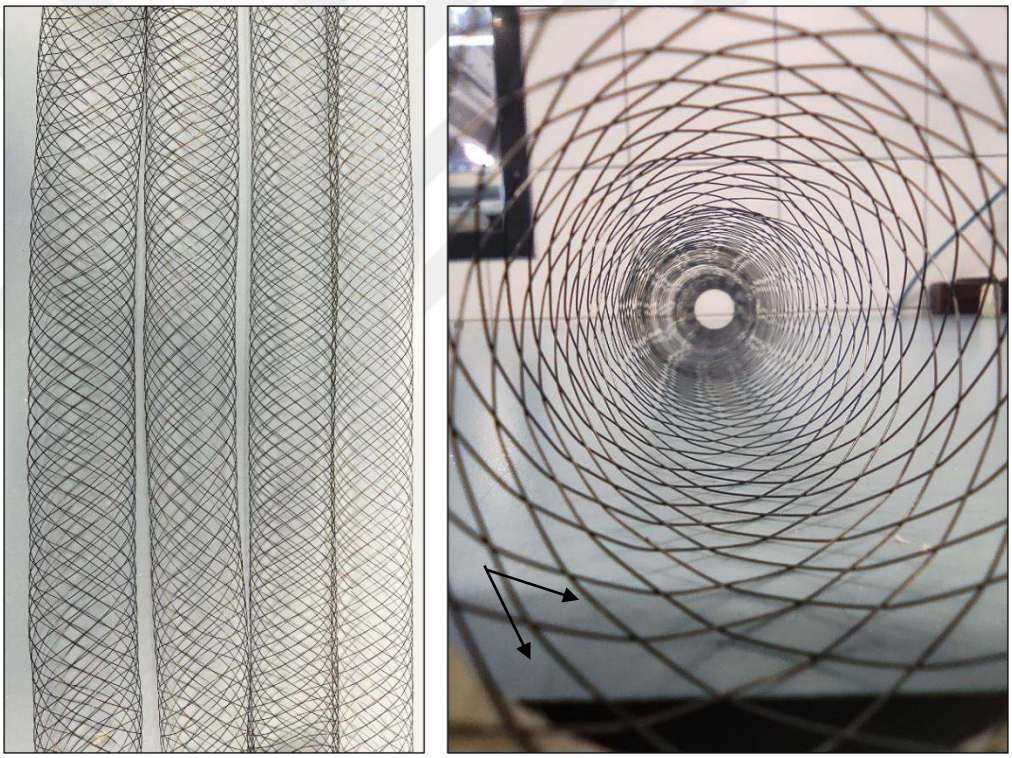

Figure 3.7. Outer and inner view of a braided stent having a 45º angle

### 3.2.5. TPU solution preparation

TPU PC 3555D from Lubrizol Corporation, Wickliffe, Ohio, United States, is used for producing nanofiber by electrospinning. To remove the residual water, TPU was dried in a vacuum oven for 24 hours at $40^0$ C. For the solution preparation, 1.137 gm TPU was used as the concentration of 8 wt% and mixed up with a 3:1 ratio of chloroform (trichloro methane) and methanol for the preparation of the solution. Later the solutions were stirred for 24 hours on a stirring plate to make the solution homogenous; after that solution was prepared for the electrospinning process.

### 3.2.6. Electrospinning

This study uses a Fluidnatek LE-500 electrospinning machine from Bionicia, Spain, to produce electrospun nanofibers. Figure 3.8 demonstrates the interior of the electrospinning setup. Parameters and settings for the electrospinning process are listed in Table 3.3. Electrospun nanofibers were covered on braided stents. Five samples have been electrospun for horizontal and vertical setups each. Ten stents have been electrospun for two braided structures using a vertical setup. For plasma and heat treatment, another ten samples have been electrospun. And aluminum foil paper is used at the edge to make the adhesion test measurement process easier. Grabbing the nanofiber would be difficult and not reproducible; that is why aluminum foil paper was used. For plasma treatment, stent samples were coated after treatment.

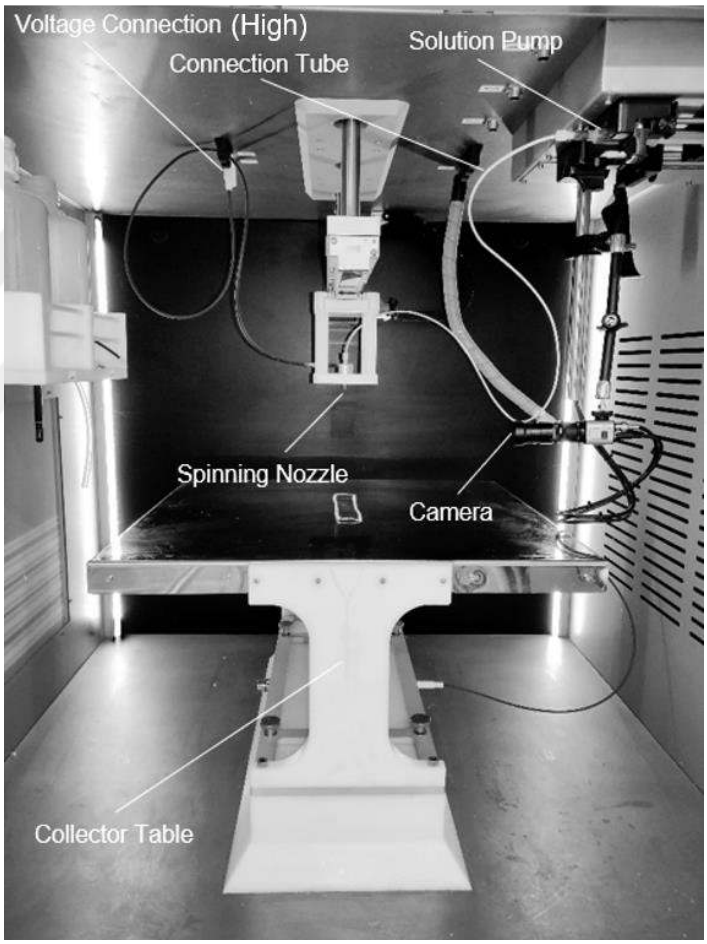


Figure 3.8. Electrospinning setup of the Fluidnatek LE-500 by Bionicia.

The machine is equipped for the coating of a single flat braided structure on a table collector. A single nozzle setup is used.

Table 3.3. Parameters used for the electrospinning process

| Parameter | Value |
|---|---|
| Voltage | ± 15 kV |
| Distance Nozzle - Collector | 200 mm |
| Flow Rate | 1.5 ml/h |
| Rotation speed | 100 rev/min |
| Rotation direction | Clockwise |
| Spinning Time | 40 min |
| Temperature | 23 °C |
| Humidity | 40 |
| Material | TPU in Trichloromethane / Methanol |
| Concentration TPU | w = 8 % |
| Nozzle diameter | 0.6 mm |

Figure 3.9 and Figure 3.10 represent the 2D and 3D structure of the braided stent before and after the electrospinning process, respectively. Here 2D samples have been done from previous project studies, and the results were collected for method validation. Initially, a 3D stent was produced with the steeger braiding machine for the flat structure of the stent. Then it was cut through lengthwise to make the 2D structure, and the edges were taped to ensure its shape. 2D stents were placed between two locked steel plates and heated for 20 minutes at 600 ° C to gain shape memory. Through the electrospinning process, TPU nanofiber was covered on the stent.

To know the differences, the 3D sample was covered with two electrospinning set up named vertical and horizontal setups based on needle position. After that, some samples were prepared for peeling tests, and some were for heat treatment.

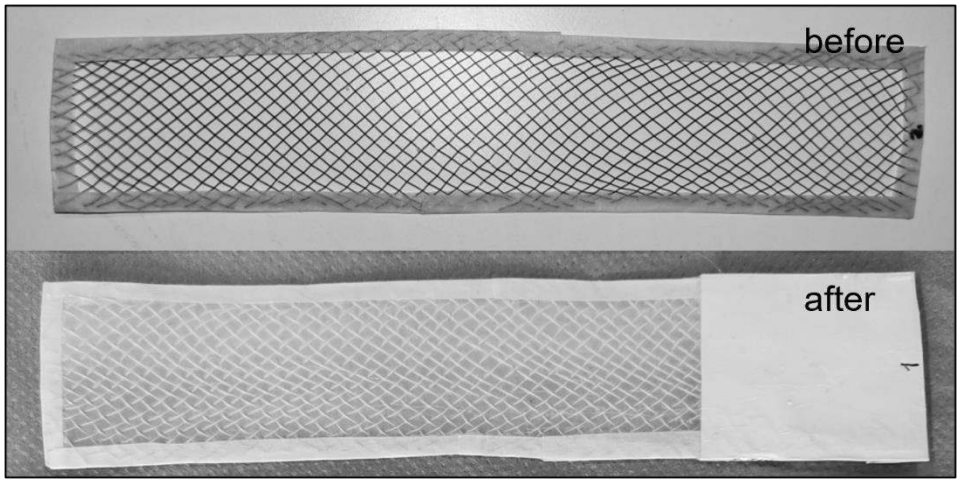


Figure 3.9. 2D braided stent before and after the electrospinning process

Figure 3.10. Braided stent before and after the electrospinning process

### 3.2.7. Adhesion test measurement of stents

Electrospun nanofiber's adhesion force to the Nitinol surface has been measured by the validated method. For the measurement, stents were cut into 5 cm lengths. The attached aluminum foil paper was clamped into the clamp and then fixed with the mandrel. Adhesive tape was used on the edge of the stent to ensure the wire did not spread out. Figure 3.11 shows the electrospun nanofiber covered stent and the adhesion force measuring process.

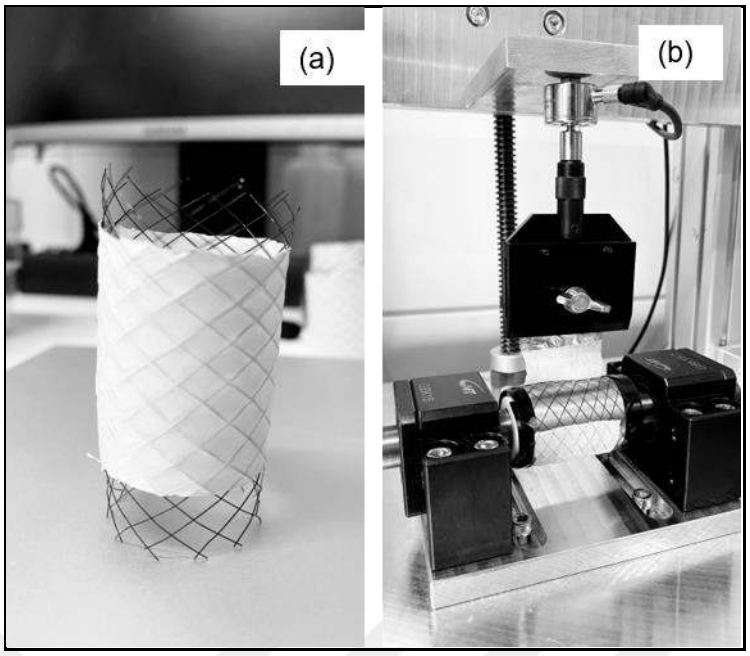


Figure 3.11. (a) nanofiber covered stent, (b) schematic view of adhesion force measurement for covered stent

### 3.2.8. Plasma treatment

To improve the adhesion force of the stent surface to electrospun nanofiber, plasma treatment was done using Pico Diener electronic plasma unit before the electrospinning process. Four distinct results might be seen when plasma is used as a treatment. The outcomes are influenced by the carrier material, gas chemistry, reactor design, and operational parameters. The four distinct consequences that happen when using plasma as a treatment are,

1) surface cleaning,
2) surface activation to improve adhesion,
3) coatings, hydrophobic and hydrophilic
4) etching.

Argon gas was used for this treatment for five minutes, and Table 3.4 shows the parameters used for this treatment. The front view of the plasma treatment machine is shown in Figure 3.12.

Table 3.4. Parameter and settings of plasma treatment used for 3D braided stent

| Parameter | Value |
|---|---|
| Power | 100 Watt |
| Gas Supply | 0,1 dl/min |
| Pressure | 0,2-0,5 mbar |
| Time | 5 min |

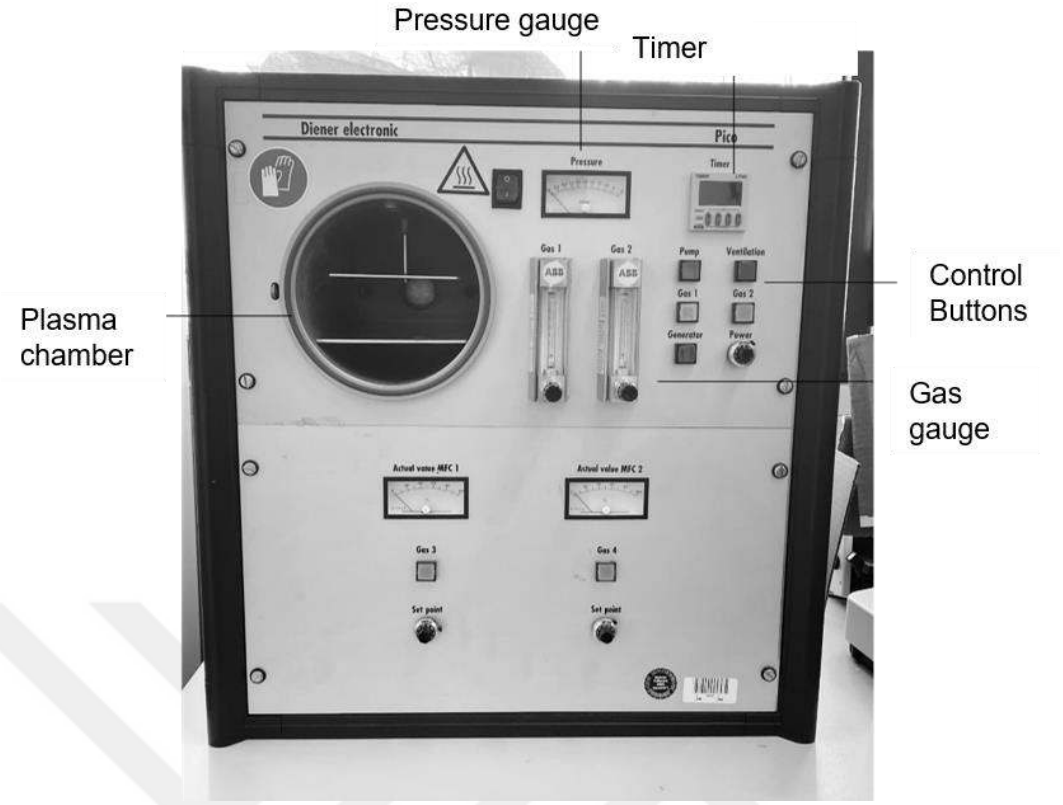


Figure 3.12. Front view of plasma unit

### 3.2.9. Heat treatment

Heat treatment has been carried out after the electrospinning process on 3D braided stents. A hot air blower from the company Herz GmbH, Neuwied, was used; for this experiment, hot air blew at $200^0$ C for around 2.5 minutes at a 5 cm distance. Since distance has a big impact on how well nanofiber heats up, an optimum distance has been selected. The nanofiber was initially treated for 1 minute at a distance of 2 cm; however, it was torn. Then, 5 cm was utilized for 1 minute, but because of the distance, the stent did not get hot; thus, 2.5 minutes was used. The rotation speed was 100 rev/min, and the stent was rotated clockwise. A schematic setup of heat treatment is shown in Figure 3.13

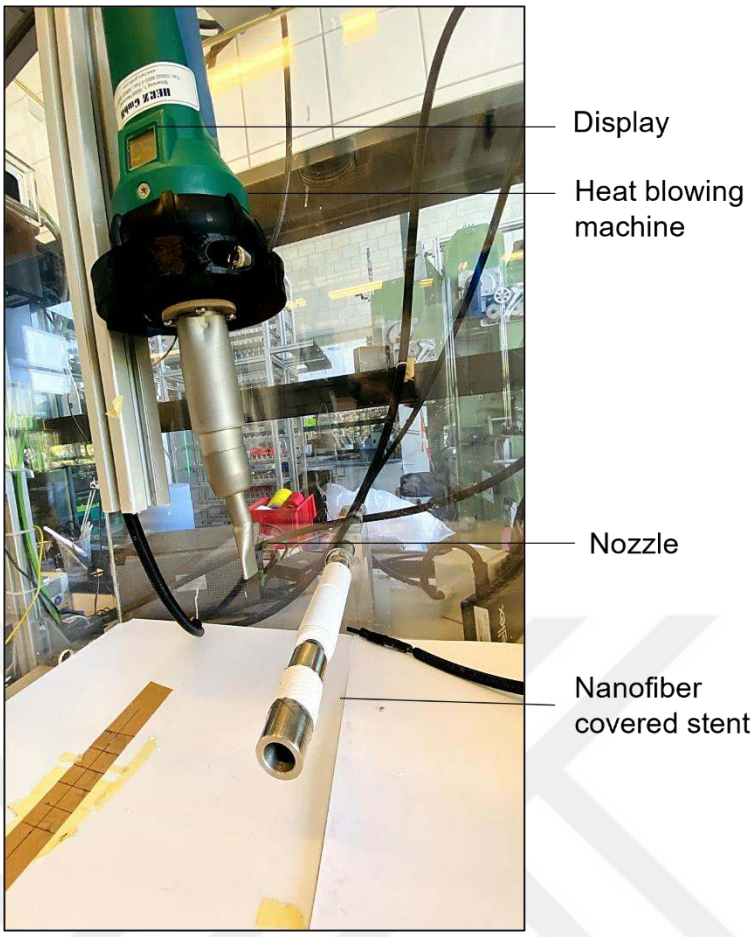

Figure 3.13. Heat-blowing machine setup for heat treatment

***Statistical analysis***

The adhesion force of the electrospun nanofiber covered stent was statistically evaluated through variance – One-way ANOVA analysis using SPSS 25.0. Statistical analysis has been done at a 95% confidence level or 0.05 significance level. If the p-value representing the significance level is less than 0.05, the difference will be statistically significant.

# 4. RESULTS AND DISCUSSIONS

## 4.1. Method validation

Three different surfaces, such as wood, steel and plastic, have been chosen for the method validation part. Peel tests have been done for 2D and 3D structures of these surfaces. Later, peel test results from the 2D sample tests by tensile testing and 3D samples test by modified machine for different adhesives were compared to find the coherent and significant difference between them. After that, the reproducibility of the test was tested. Test results of different surfaces are described below.

### 4.1.1. Wood surface

Six types of adhesives have been used for wood surfaces. Figure 4.1 to Figure 4.6 represent the results that have been found from this study. From Figure 4.1, it is demonstrated that, for 3D samples, Fmax and Favg are higher than in 2D samples, while Fmin is lower than in 2D samples. It observes that 3D samples have 1.35 and 1.41 times higher Fmax and Favg than 2D samples. 0.87 times minimum force is observed for the 3D wood sample for tape 1.

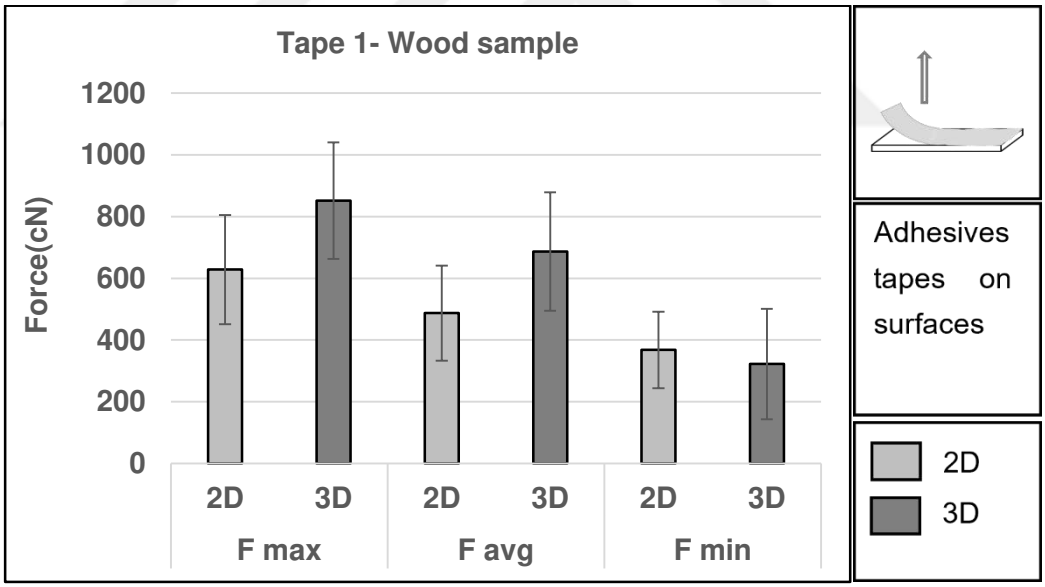


Figure 4.1. Forces of 2D and 3D wood surfaces for Tape 1

Figure. 4.2 illustrates the maximum, average and minimum results of forces on 2D and 3D wood surfaces due to tape 2. From the figure, it is observed that 3D wood surfaces have 1.26, 1.26 and 1.15 times higher Fmax, Favg and Fmin than 2D wood surfaces, respectively.

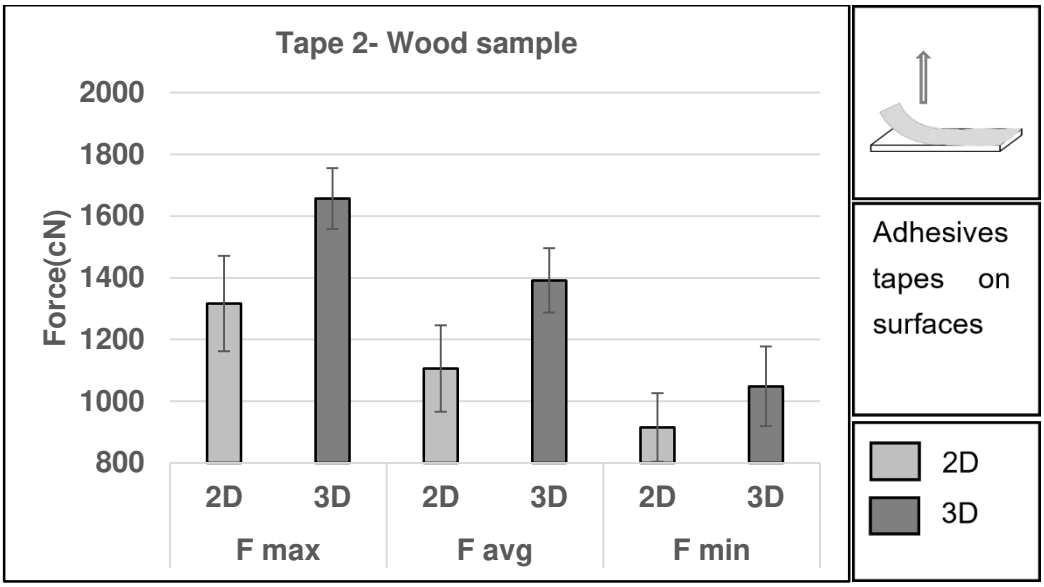


Figure. 4.2. Forces of 2D and 3D wood surfaces for Tape 2

Forces for tape 3 in wood surfaces are indicated in Figure 4.3. The figure depicts that 2D samples have higher forces than 3D samples. From the experimental results, it has been found that 2D wood surfaces have 1.63, 1.52 and 1.94 times higher Fmax, Favg, and Fmin than 3D wood surfaces, respectively.

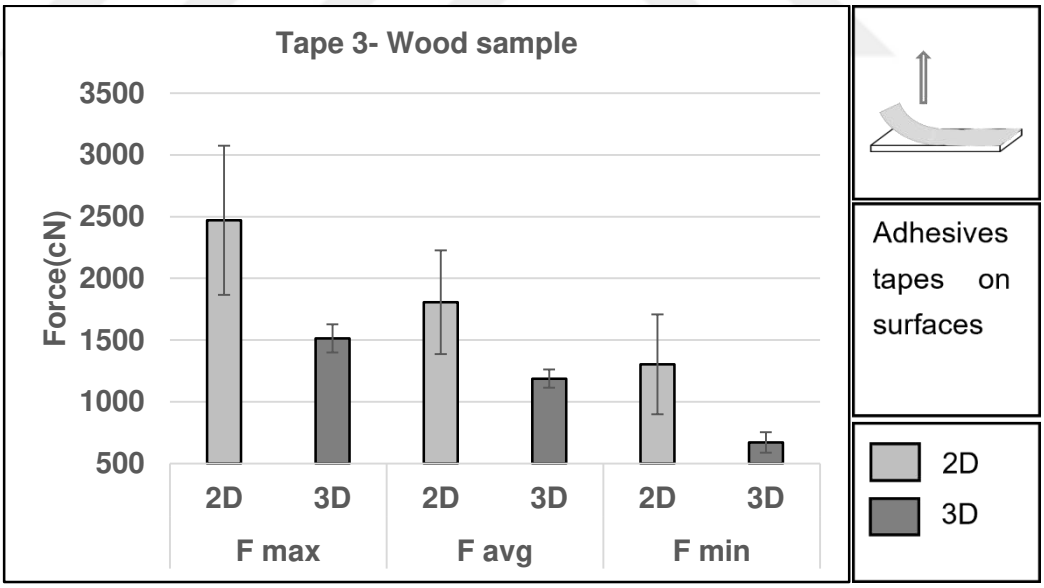


Figure 4.3. Forces of 2D and 3D wood surfaces for Tape 3

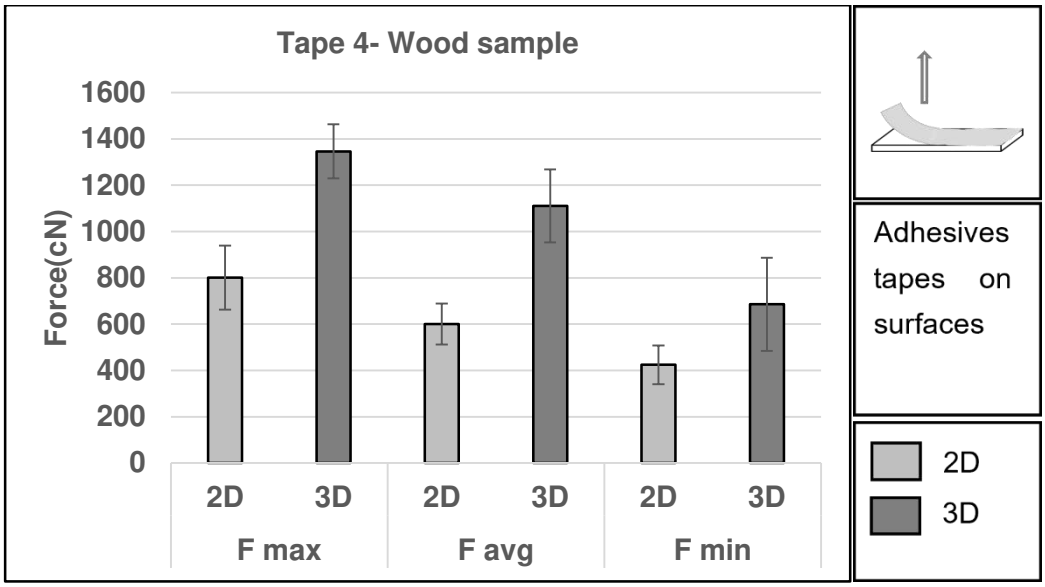


Figure 4.4. Forces of 2D and 3D wood surfaces for Tape 4

Figure 4.4 represents the forces of 2D and 3D wood surfaces for tape 4. From the figure, it is observed that 2D wood surfaces show lower forces than 3D wood surfaces. 1.68, 1.85, and 1.61 times higher Fmax, Favg and Fmin are observed for 3D wood surfaces compared to 2D wood surfaces for tape 4.

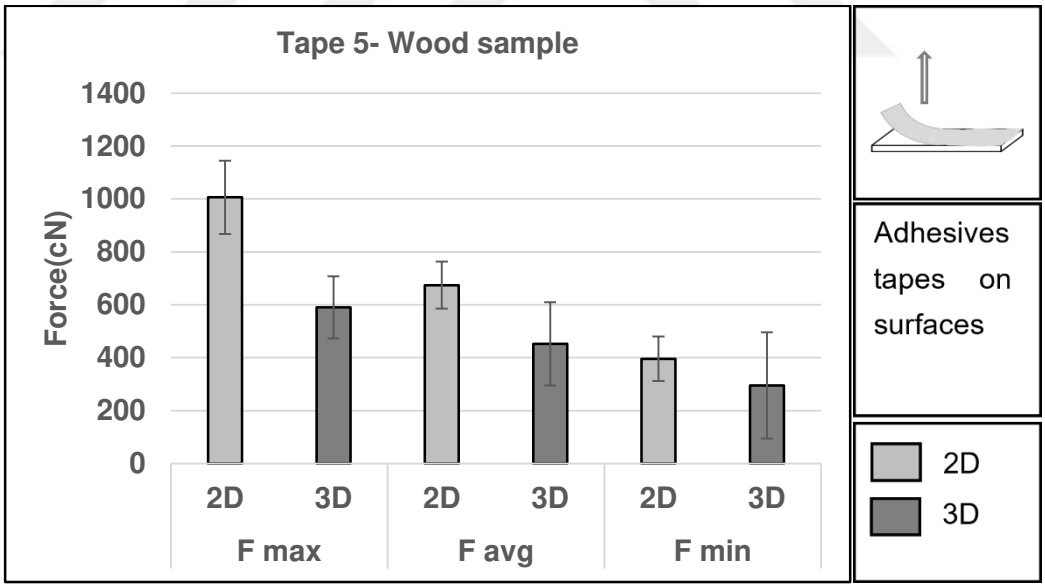


Figure 4.5. Forces of 2D and 3D wood surfaces for Tape 5

Figure 4.5 represents the forces of wood samples of 2D and 3D surfaces for tape 5. Here it is observed that 2D samples have a higher amount of force than 3D samples. Forces have been decreased 0.58, 0.67 and 0.75 times from 2D to 3D samples for Fmax, Favg and Fmin, respectively.

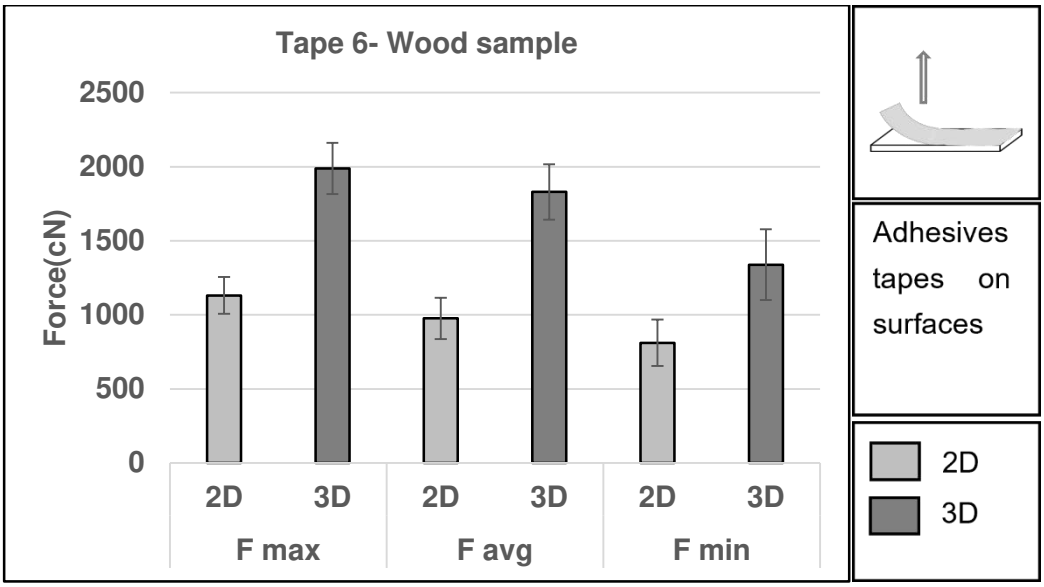


Figure 4.6. Forces of 2D and 3D wood surfaces for Tape 6

Forces for tape 6 have been shown in Figure 4.6. From the figure, it is observed that 3D wood surfaces show higher forces than 2D wood surfaces, and it is 1.75, 1.87 and 1.65 times higher for Fmax, Favg and Fmin, respectively.

### 4.1.2. Steel surfaces

For the steel surfaces, the experimental results of the peel test have been shown in Figure 4.7 to Figure. 4.12. Figure 4.7 depicts the forces for tape 1. It is found that 3D steel surfaces have slightly higher forces than 2D surfaces, and it is nearly 1.05 times.

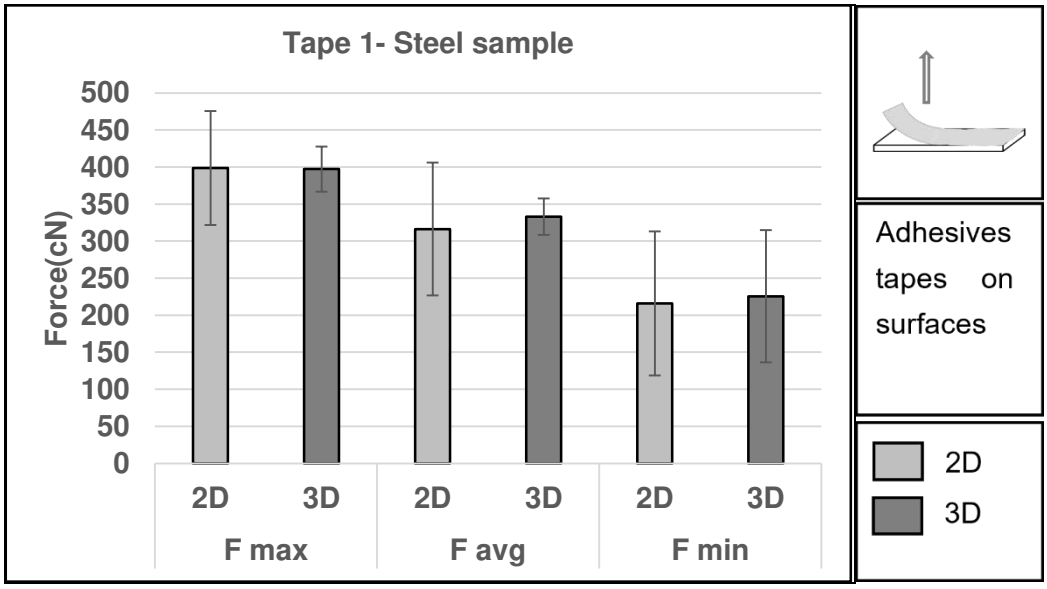


Figure 4.7. Forces of 2D and 3D steel surfaces for Tape 1

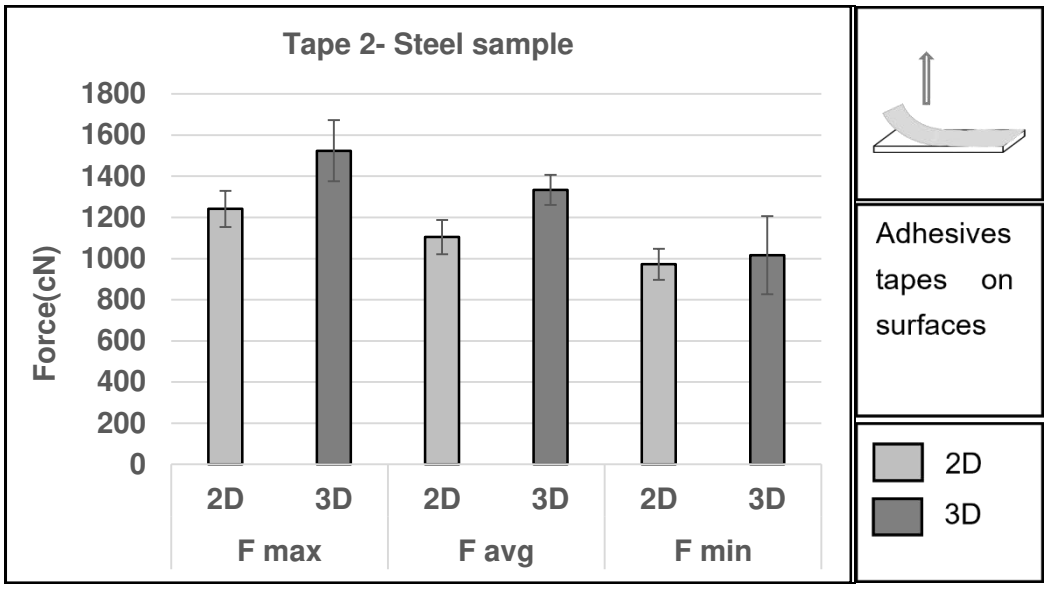


Figure 4.8. Forces of 2D and 3D steel surfaces for Tape 2

Figure 4.8 represents the forces of steel samples of 2D and 3D surfaces for tape 2. Here it is observed that 3D samples have a higher amount of force than 2D samples. Forces have been increased 1.23, 1.21 and 1.1 times from 3D to 2D samples for Fmax, Favg and Fmin, respectively.

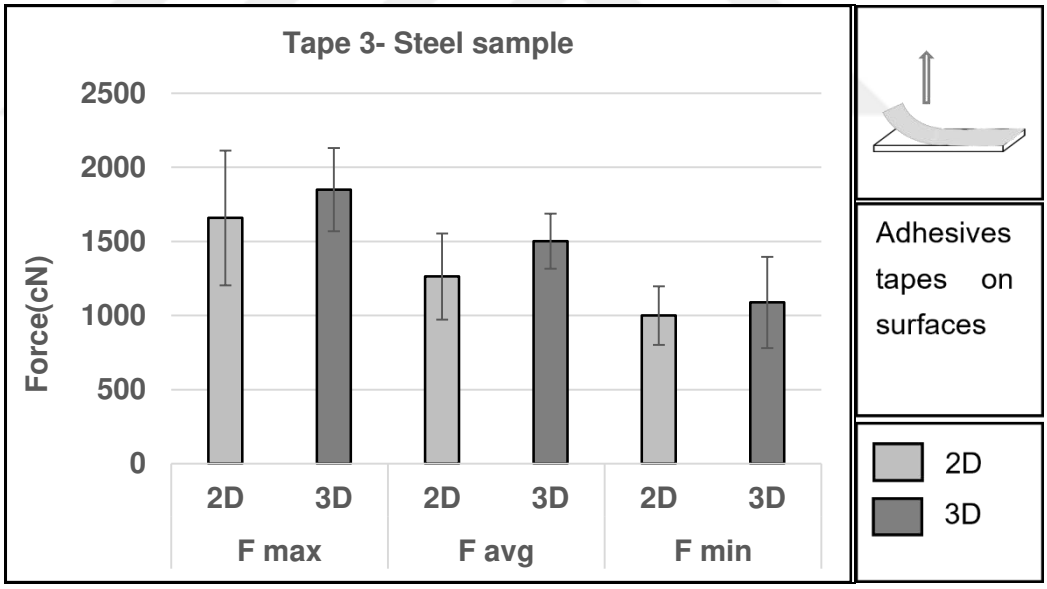


Figure 4.9. Forces of 2D and 3D steel surfaces for Tape 3

Forces for tape 3 in steel surfaces are indicated in Figure 4.9. The figure depicts that 3D steel samples have slightly higher forces than 2D steel samples. From the experimental results, it has been found that 3D steel surfaces have 1.12, 1.19 and 1.1 times higher Fmax, Favg, and Fmin than 2D steel surfaces, respectively, for tape 3.

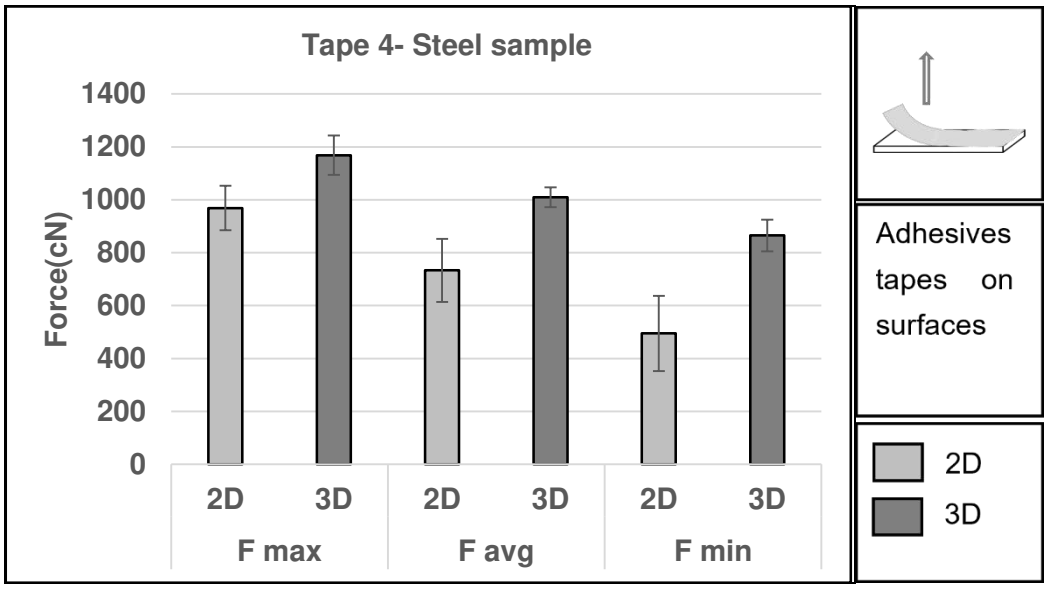


Figure 4.10. Forces of 2D and 3D steel surfaces for Tape 4

From Figure 4.10, it is demonstrated that, for 3D samples, Fmax, Favg and Fmin are higher than in 2D samples. It observes that 3D samples have 1.21, 1.38 and 1.75 times higher Fmax, Favg, and Fmin than 2D samples.

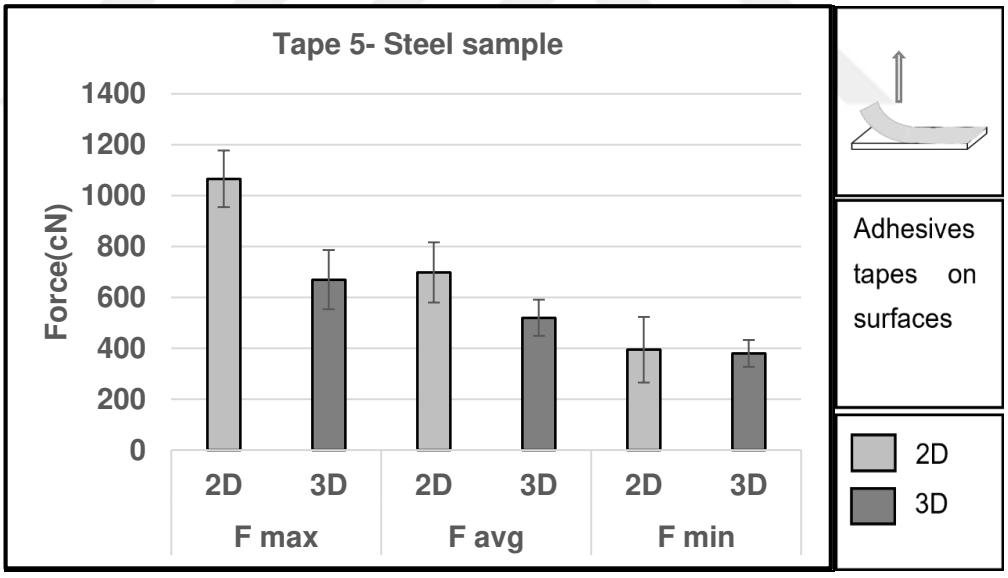


Figure 4.11. Forces of 2D and 3D steel surfaces for Tape 5

Figure 4.11 illustrates the maximum, average and minimum results of forces on 2D and 3D steel surfaces due to tape 5. From the figure, it is observed that 3D steel surfaces have 0.63, 0.74 and 0.96 times lower Fmax, Favg, and Fmin than 2D steel surfaces, respectively.

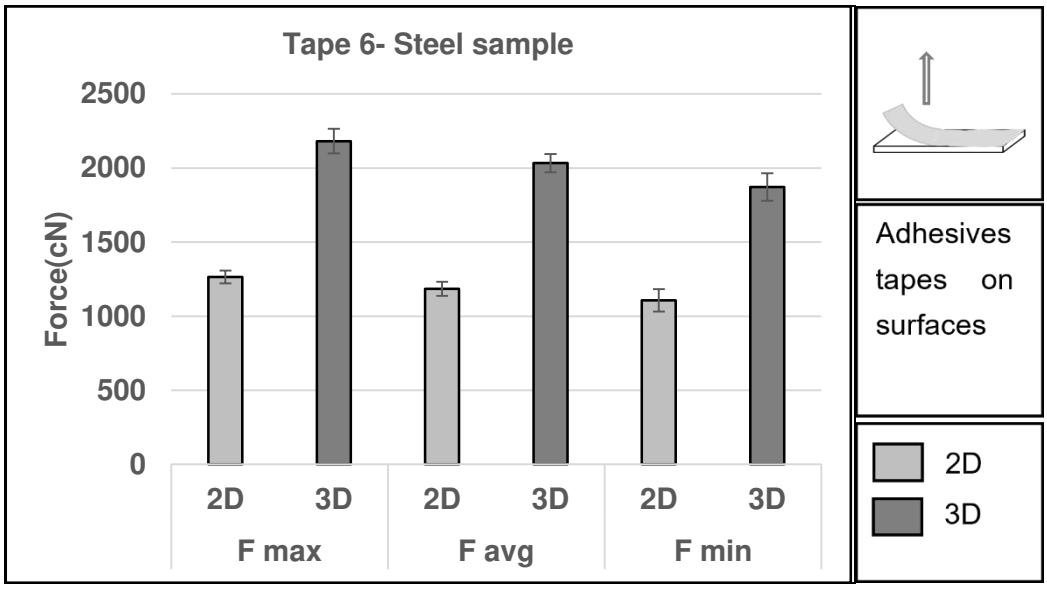


Figure 4.12. Forces of 2D and 3D steel surfaces for Tape 6

Forces for tape 6 in steel surfaces are indicated in Figure 4.12. The figure depicts that 3D samples have higher forces than 2D samples. The experimental results show that 3D steel surfaces have 1.72, 1.72 and 1.69 times higher Fmax, Favg, and Fmin than 2D steel surfaces.

### 4.1.3. Plastic surfaces

Figure 4.13 to Figure 4.18 shows the maximum, average and minimum forces of 2D and 3D plastic surfaces for tape 1 to tape 6. Figure 4.13 shows that 2D plastic surfaces have slightly higher forces than 3D samples. For tape 1, 3D plastic surfaces have 0.80, 0.84 and 0.88 times lower Fmax, Favg, and Fmin than 2D plastic samples.

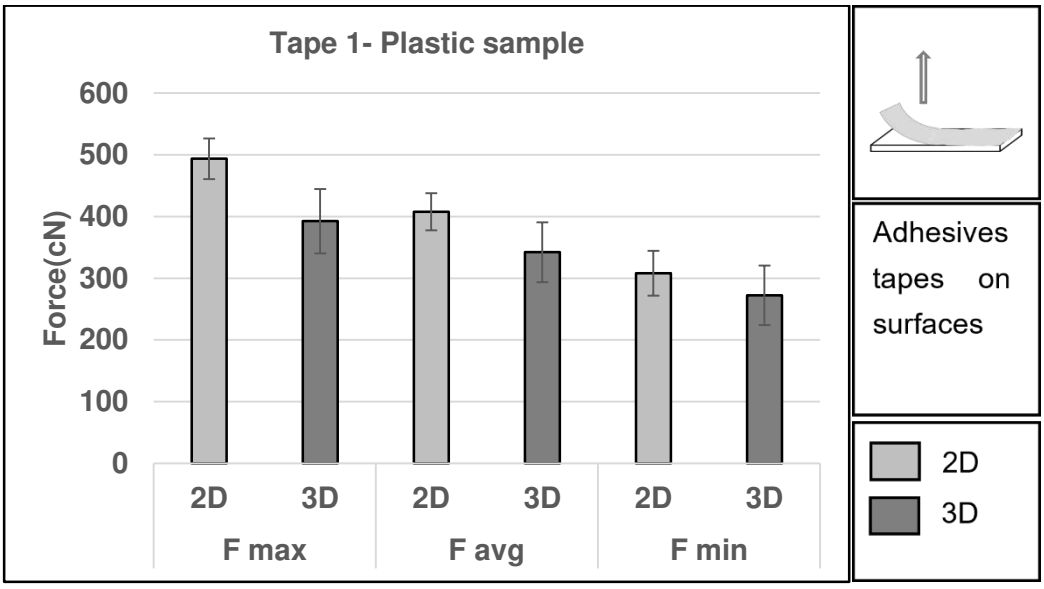


Figure 4.13. Forces of 2D and 3D steel surfaces for Tape 1

Forces for tape 2 in plastic surfaces are indicated in Figure 4.14. The figure depicts that 3D plastic samples have higher forces than 2D plastic samples. From the experimental results, it has been found that 3D plastic surfaces have 1.68, 1.71 and 1.50 times higher Fmax, Favg, and Fmin than 2D plastic surfaces, respectively, for tape 2.

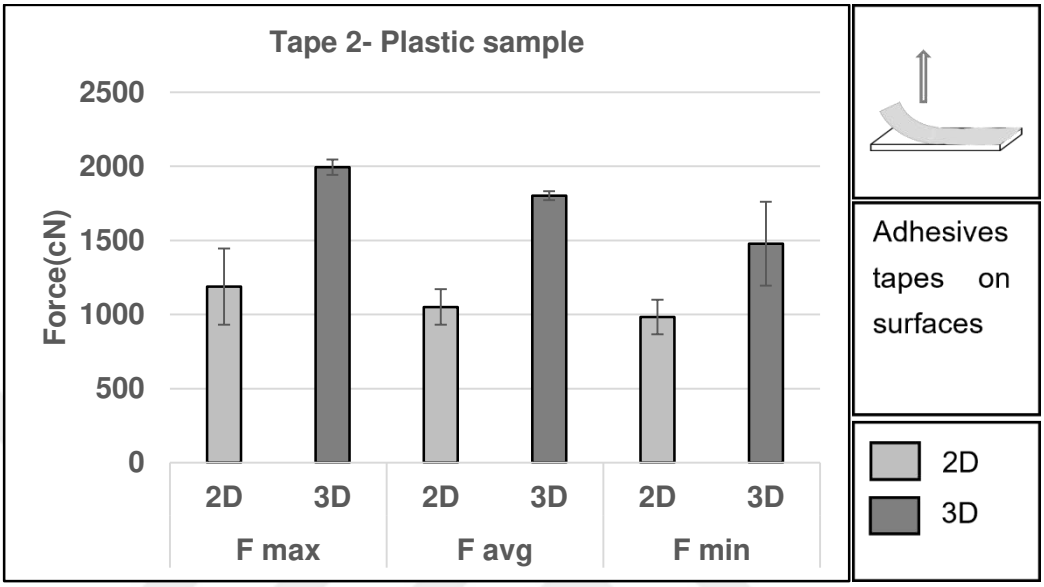


Figure 4.14. Forces of 2D and 3D steel surfaces for Tape 2

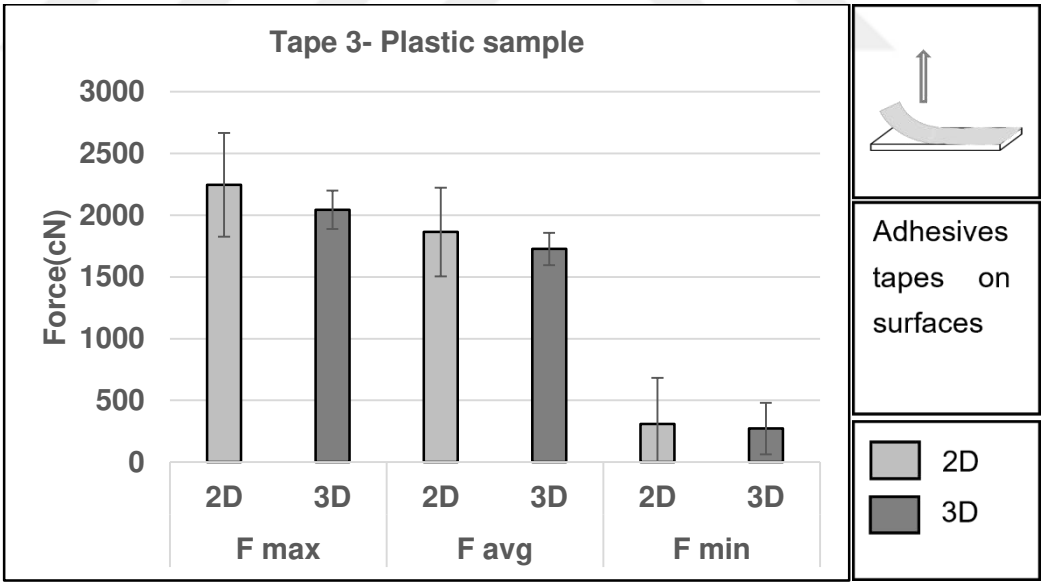


Figure 4.15. Forces of 2D and 3D steel surfaces for Tape 3

Figure 4.15 represents the forces of plastic samples of 2D and 3D surfaces for tape 3. Here it is observed that 3D samples have less force than 2D samples. Forces have been decreased 0.91, 0.93 and 0.88 times from 2D to 3D plastic samples for Fmax, Favg and Fmin, respectively.

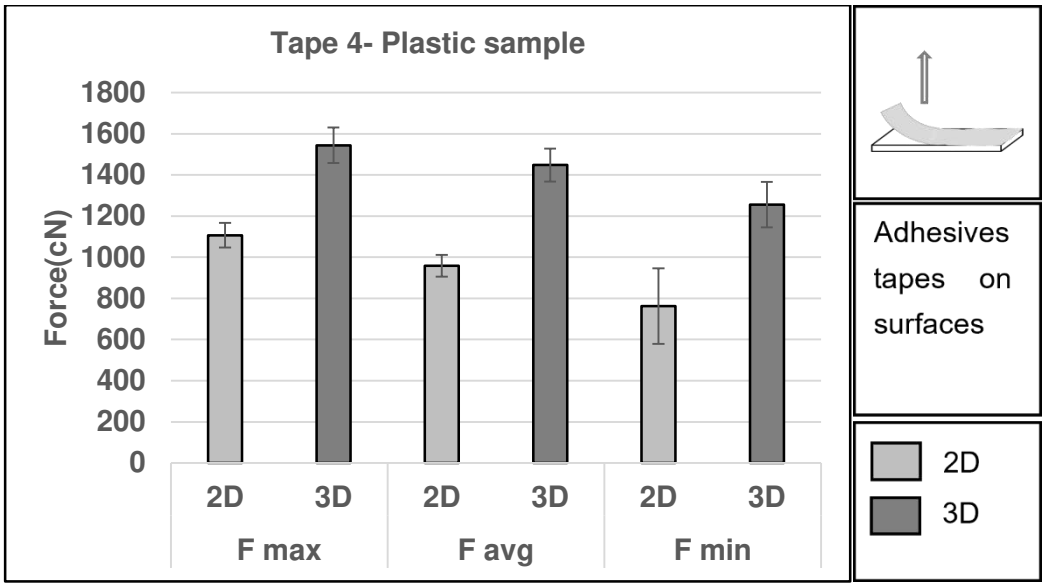


Figure 4.16. Forces of 2D and 3D steel surfaces for Tape 4

Figure 4.16 represents the forces of plastic samples of 2D and 3D surfaces for tape 4. Here it is observed that 3D samples have more force than 2D samples. Forces have been increased 1.39, 1.51 and 1.65 times from 2D to 3D samples for Fmax, Favg and Fmin, respectively.

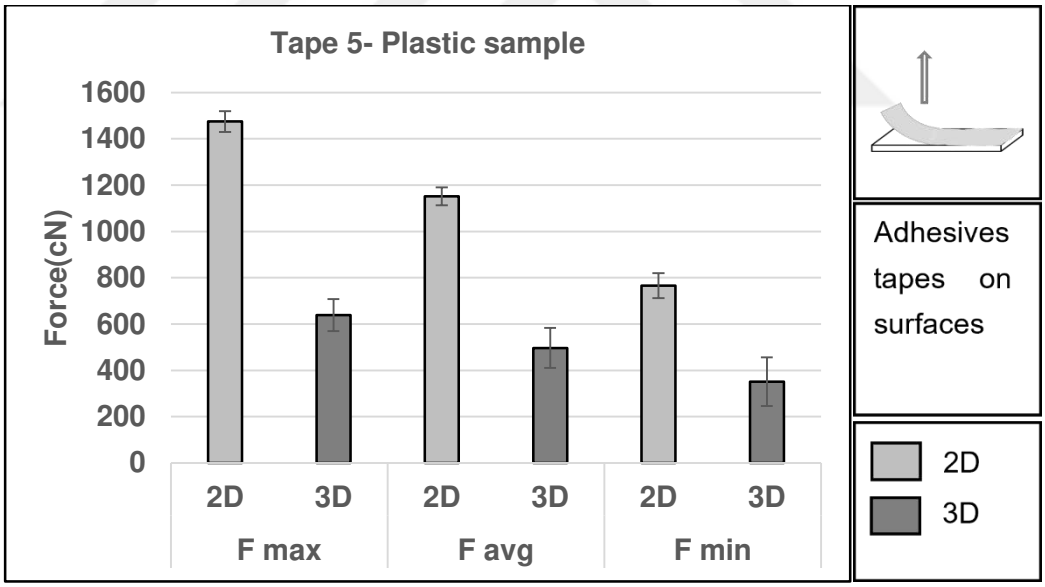


Figure 4.17. Forces of 2D and 3D steel surfaces for Tape 5

Figure 4.17 illustrates the maximum, average and minimum results of forces on 2D and 3D plastic surfaces due to tape 5. The figure shows that 3D wood surfaces have almost half times Fmax, Favg, and Fmin as 2D wood surfaces.

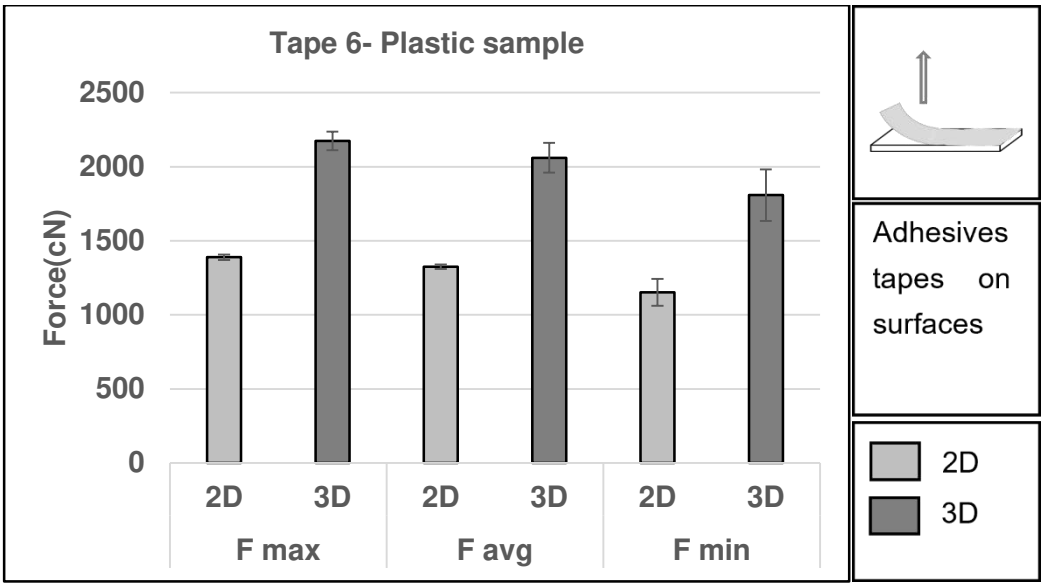


Figure 4.18. Forces of 2D and 3D steel surfaces for Tape 6

Forces for tape 6 on plastic surfaces have been shown in Figure 4.18. From the figure, it is observed that 3D plastic surfaces show higher forces than 2D plastic surfaces, which are 1.57, 1.55 and 1.57 times higher for Fmax, Favg and Fmin, respectively.

### 4.1.4. Key findings

From the experimental results of 2D and 3D structured surfaces for the tapes, it can be observed that adhesion forces are changed almost coherently for different surfaces. Sometimes high standard variation has been observed, possibly due to factors like sample preparation as it had different surfaces and adhesive tapes.

Another factor was human error, or the pressure applied before the test. Also, handling the samples affected the results, which caused high variation. The overall adhesion force relation of 2D and 3D has been shown in Tab. 4.1. From the table, it is observed that a coherent adhesion force from 2D to 3D surfaces. For Tape 2,4, and 6, all the surfaces show 1.1 to up to 1.7 times higher results from 2d to 3D surfaces. Tape 5 shows up to 0.9 times the results from 2d to 3D surfaces. Overall, the adhesion force for 3D samples is observed to be 0.7 to 1.7 times. That indicates that the modified method is valid for measuring the 3D structured surface's adhesion force.

Table 4.1. Relation of adhesion forces for different 2D and 3D structured surfaces

| Surface | Adhesive | Adhesion force from 2D to 3D |
|---|---|---|
| Steel | Tape 1, 2, 3, 4, 6 | 1.1 - 1.7 times increased |
| | Tape 5 | up to 0.7 times decreased |
| Wood | Tape 1, 2, 4, 6 | 1.2 - 1.7 times increased |
| | Tape 3, 5 | up to 0.7 times decreased |
| Plastic | Tape 2, 4, 6 | 1.4 - 1.7 times increased |
| | Tape 1, 3, 5 | up to 0.9 times decreased |

### 4.1.5. Reproducibility

To validate a method, it is necessary to check the reproducibility of the method. In this study, two persons did the adhesion test separately by following the same method described in the 3D peel test part for steel surfaces with tape 6 without any influence from the other person for the modified 3D adhesion force testing machine. Surface and adhesive tape were chosen randomly. Figure 4.19 represents the reproducibility results of the modified machine. The figure shows that Fmax, Favg and Fmin are quite similar for the two persons. From the statistical analysis, it is found that Fmin has no statistically significant difference for the two persons though there is a significant difference for Fmax and Favg.

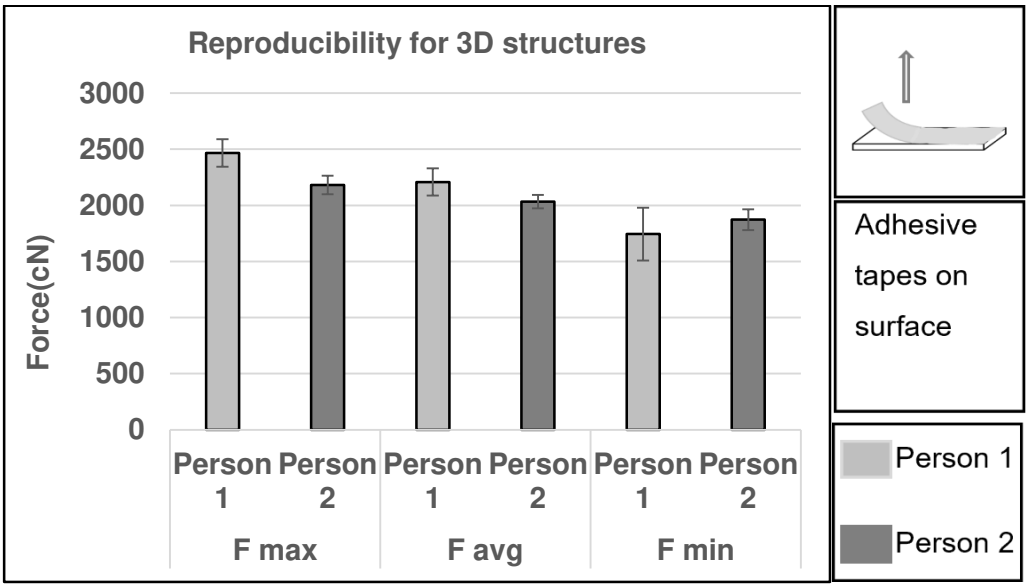


Figure 4.19. Reproducibility of adhesion force test for 3D structured samples

## 4.2. 2D vs. 3D stent

2D and 3D structured braided stents have been produced and covered using TPU electrospun nanofiber. Parameters and settings of the braiding machine and electrospinning machine have been

described in the method chapter and kept similar for both surfaces. For this study, a vertical electrospinning setup has been used for both 2D and 3D structured stents. The figure shows that 3D stents have a slightly higher amount of force than 2D samples. 3D samples have 1.38, 1.34 and 1.43 times higher adhesion force than 2d samples for Fmax, Favg and Fmin, respectively. That means the adhesion force is increased roughly 1.4 times from 2D to 3D structured samples, comparable to other previously described surfaces. It was observed that the adhesion force was increased almost 1.1 to 1.7 times for the different surfaces with different adhesive tapes. Here electrospun covered stents also follow the range from 2D to 3D structure. From the One-Way ANOVA statistical test, at the significance level of 0.05, no statistically significant differences have been found for the Fmax, Favg, and Fmin between 2D and 3D samples. This result indicated that the modified method is able used for measuring the adhesion force of nanofiber on 3D cylindrical stents.

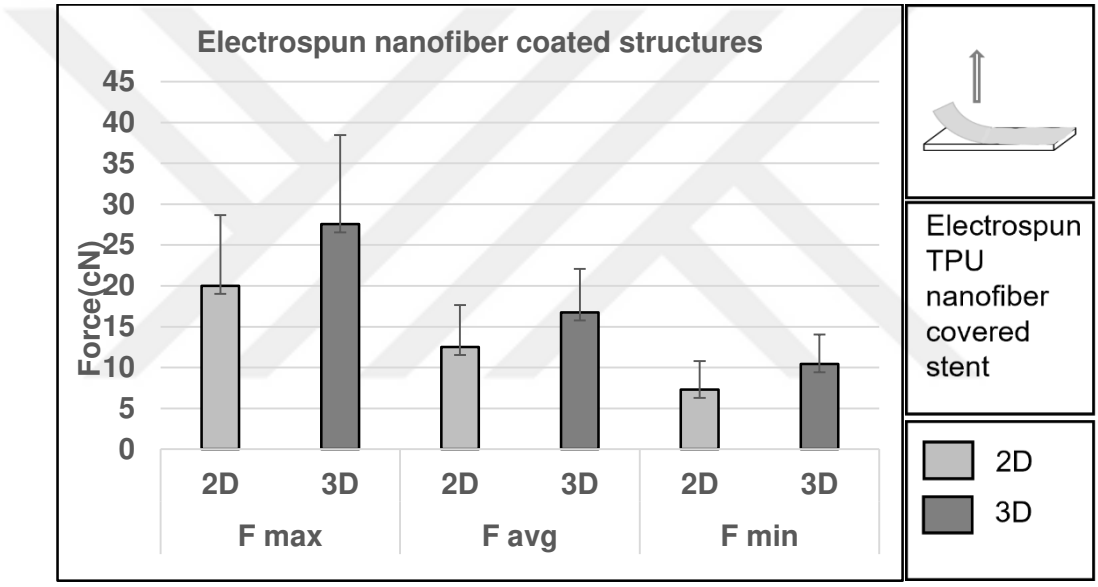


Figure 4.20. Adhesion forces of 2D and 3D braided structured electrospun TPU nanofiber covered stent

### 4.3. Adhesion force of differently braided stents

Two distinct forwarding speeds have been chosen in order to assess the effect of the adhesion force at various forwarding speeds on braided electrospun covered stents. 2 and 5 picks/cm (pix/cm) were two different forwarding speeds. These two different forwarding speeds influence stent structures. Higher forwarding speed makes the stent denser as it increases the wire density per centimeter (cm). Figure 4.21 depicts the adhesion force of differently braided stents. In this study, it is observed that a higher forwarding speed shows higher adhesion force. Having a denser structure is one reason for that, as nanofiber can attach more to the stent surface and thus increase the forces. From the figure, it is depicted that, having 5 pix/cm forwarding speed in the braiding machine, Fmax, Favg and Fmin are increased roughly 1.22, 1.47 and 1.74 times, respectively, then having 2 pix/cm forwarding speed.

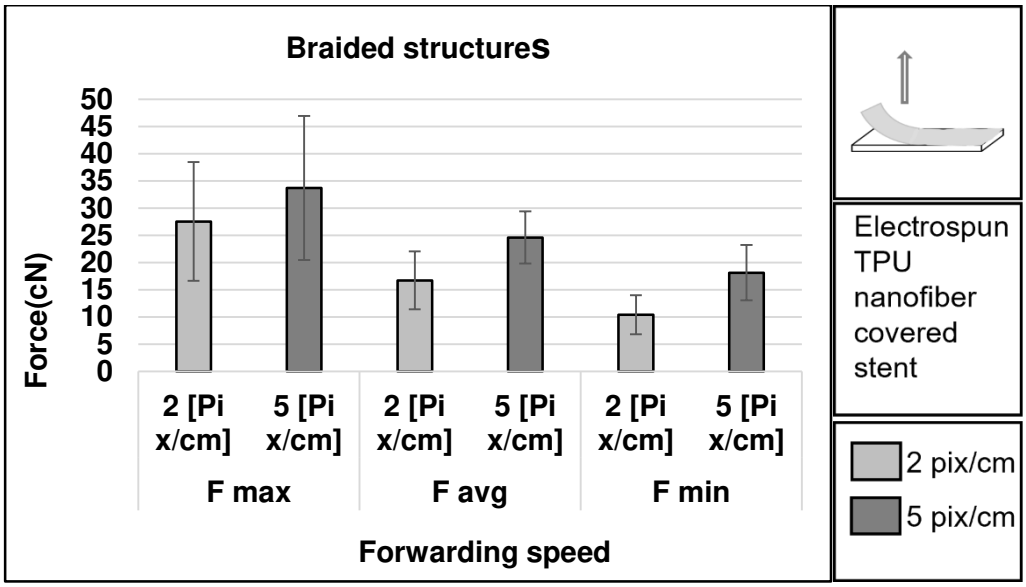


Figure 4.21. Adhesion force of differently braided (forwarding speed) stents

### 4.4. Adhesion force of different electrospinning setup

Two electrospinning systems have been used to understand the effect of needle position in the electrospinning process on the adhesion force of electrospun nanofiber covered stent. Vertical and horizontal setups have been used for this study, and Figure 4.22 represents the adhesion forces of vertically, and horizontally electrospun nanofiber covered nitinol stents. The figure shows, that the maximum average force of these two setups is quite similar, though $F_{avg}$ and $F_{min}$ are almost 1.5 times higher for horizontal setup than vertical setup. No statistically significant differences have been observed for the different setups at a significant level of 0.05.

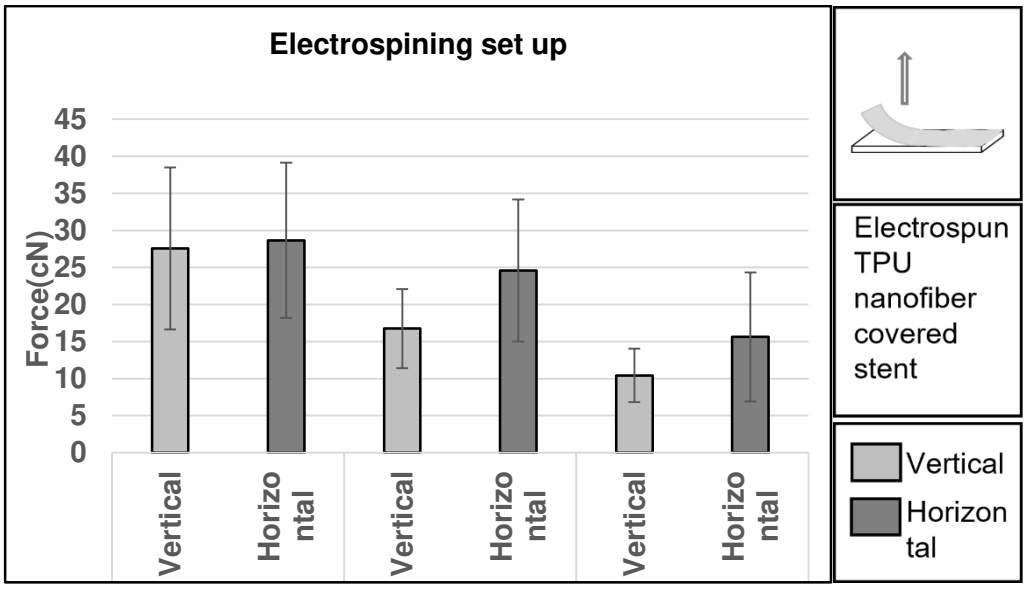


Figure 4.22. Adhesion force for different electrospinning setups

### 4.5. Adhesion force of treated stents

The adhesion force between electrospun nanofiber and nitinol stent is not quite enough; that is why an increased adhesion force is required between them for better performance. To get enhanced results, in this study, stents were treated with plasma and heat treatment, and the process is described in the method chapter. Figure 4.23 demonstrates the adhesion force of treated stents and compares the results with reference samples that are not treated. From the results, it is found that plasma-treated stents show better adhesion force than others. For plasma treatment, adhesion forces are increased roughly 1.98, 2.5 and 2.17 times more for $F_{max}$, $F_{avg}$ and $F_{min}$, respectively, than in reference one. Nanofibers adhere strongly and produce substantial adhesion forces as a result of plasma treatment because it deposits ions on the surfaces. On the other hand, for the heat treatment, $F_{max}$, $F_{avg}$ and $F_{min}$ are 1.58, 1.58 and 1.62 times higher than the reference stent. Due to heat, the nanofiber tried to shrink, which helped attach to the stent surface, but there was no chemical attachment to increase the adhesion force.

According to One-way ANOVA statistical analysis, it is found there are only statistically significant differences between reference and plasma-treated stents. No statistically significant difference between reference and heat-treated stents and heat and plasma-treated stents has been observed.

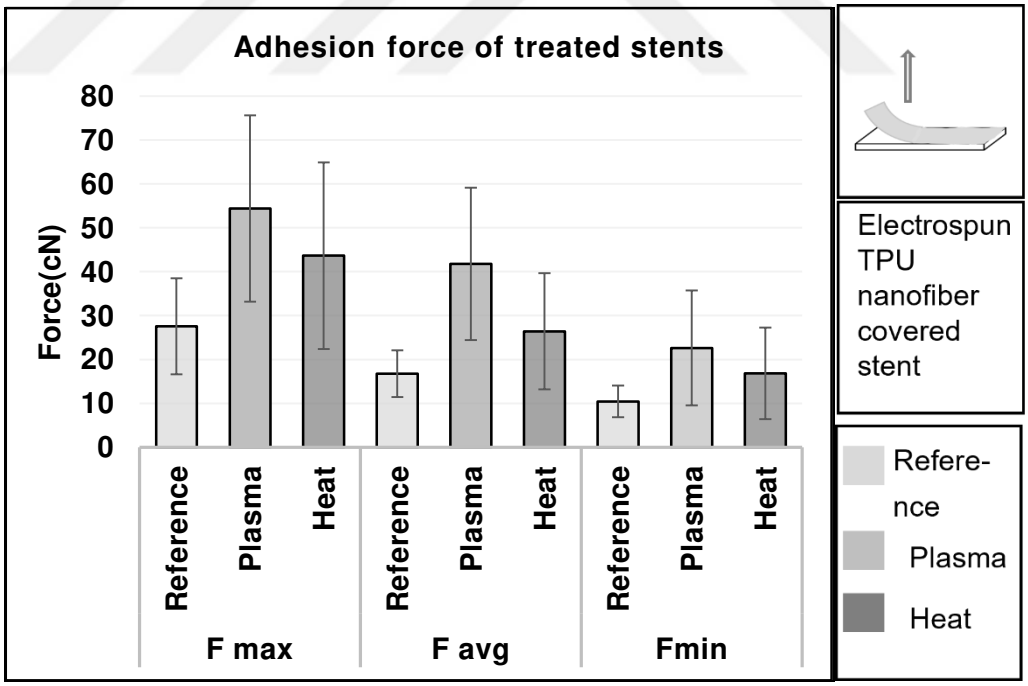


Figure 4.23. Adhesion force of treated stents

## 5. CONCLUSIONS

This work aims to validate a method for measuring the adhesion force of electrospun nanofiber covered nitinol stent. In the first part of this study, three different- wood, steel and plastic surfaces were used with six different types of adhesive tapes. The adhesion force of 2D surfaces was measured using a tensile testing machine, and for 3D surfaces modified machine was used. The results found from these tests were then compared for the same surfaces and tapes. According to the experimental findings, adhesion forces between 2D and 3D surfaces increased by 1.2 to 1.7 times and dropped by up to 0.7 times per various surfaces and tapes. Having coherent results validated the method for measuring the adhesion force of 3D structured samples. Later, two users used the modified equipment to perform the adhesion force test with adhesive tape on a specific surface in order to ensure the method's reproducibility. For this, all the procedures were the same rather than users. The outcomes showed that the modified machine is verified and the procedure is reproducible.

To evaluate the validated method for nanofiber covered stents, the adhesion force between electrospun nanofiber covered 2D and 3D structured stents was also measured. Results were quite similar to the previous results of different surfaces of 2D to 3D structures. The adhesion force increased from 2D to 3D stent structure roughly 1.4 times which is comparable to other surfaces. These results illustrated that the modified machine could be used to measure the adhesion force of the electrospun covered stent. Since the modified machine used the normal norm for the 3D samples, and the tested findings were consistent with those of the 2D samples, it can be said that the procedure is reliable.

Later in this study, the adhesion force of the electrospun nanofiber covered stents surface was evaluated in terms of different braiding structures, electrospinning set up and treatment. On average, having a higher wire density in the braiding structure exerted nearly 1.5 times higher adhesion force than having a lower wire density. Regarding the electrospinning setup, the horizontal setup showed roughly 1.5 times higher adhesion force for the electrospun nanofiber covered stent. Plasma and heat treatment was applied to the stent to improve the adhesion force between the nanofiber and stent. It was found that adhesion forces have been increased more than 2 times than untreated reference stent, while heat treatment showed more than 1.5 times increasement.

It can be noted that to get a better adhesion force, plasma treatment is a good option. Though there was a lot of variation in results observed in the modified machine for 3D cylindrical structured adhesion force, these can be overcome by implementing different sensors and attachments in the machine. For example, holding the edge of the stent would be beneficial, as using tape hampers the nanofiber covering. Also, a flexible sliding mandrel is required for flexible clamping and overcoming material handling. Moreover, further study could be done in terms of using different braiding angles and braiding parameters at the braiding stage. Focusing on stent structure and materials would be another scope of this study for measuring adhesion force and evaluating it. It is also possible to

examine the adhesion performances using various biocompatible polymers such as nanofiber and various treatments.

## REFERENCES


American Heart Association. (2017). What Is a Stent? *ANSWERS by Heart*, 2. https://www.heart.org/idc/groups/heart-public/@wcm/@hcm/documents/downloadable/ucm_300452.pdf

Ang, H. Y., Ng, J., Bulluck, H., Wong, P., Venkatraman, S., Huang, Y., & Foin, N. (2018). Fundamentals of bioresorbable stents. In *Functionalised Cardiovascular Stents* (pp. 75–97). Elsevier. https://doi.org/10.1016/B978-0-08-100496-8.00005-6

Bhardwaj, N., & Kundu, S. C. (2010). Electrospinning: A fascinating fiber fabrication technique. *Biotechnology Advances*, *28*(3), 325–347. https://doi.org/10.1016/j.biotechadv.2010.01.004

Chong, E. J., Phan, T. T., Lim, I. J., Zhang, Y. Z., Bay, B. H., Ramakrishna, S., & Lim, C. T. (2007). Evaluation of electrospun PCL/gelatin nanofibrous scaffold for wound healing and layered dermal reconstitution. *Acta Biomaterialia*, *3*(3 SPEC. ISS.), 321–330. https://doi.org/10.1016/j.actbio.2007.01.002

Esfahani, H., Jose, R., & Ramakrishna, S. (2017). Electrospun ceramic nanofiber mats today: Synthesis, properties, and applications. *Materials*, *10*(11). https://doi.org/10.3390/ma10111238

Fong, H., & Reneker, D. H. (1999). Elastomeric Nanofibers of Styrene-Butadiene-Styrene Triblock Copolymer. In *J Polym Sci B: Polym Phys* (Vol. 37).

Heo, D. N., Lee, J. B., Bae, M. S., Hwang, Y. S., Kwon, K. H., & Kwon, I. K. (2011). Development of nanofiber coated indomethacin-eluting stent for tracheal regeneration. *Journal of Nanoscience and Nanotechnology*, *11*(7), 5711–5716. https://doi.org/10.1166/jnn.2011.4495

Huang, Z. M., Zhang, Y. Z., Kotaki, M., & Ramakrishna, S. (2003). A review on polymer nanofibers by electrospinning and their applications in nanocomposites. *Composites Science and Technology*, *63*(15), 2223–2253. https://doi.org/10.1016/S0266-3538(03)00178-7

J. Guerra, A., & Ciurana, J. (2009). *Nanofiber Covered Stent For Vascular Diseases*. 1–162.

J. Guerra, A., & Ciurana, J. (2019). Stent's Manufacturing Field: Past, Present, and Future Prospects. *Angiography*, *4*. https://doi.org/10.5772/intechopen.81668

Jamshidi, P., Mahmoody, K., & Erne, P. (2008). Covered stents: A review. *International Journal of Cardiology*, *130*(3), 310–318. https://doi.org/10.1016/j.ijcard.2008.04.083

Kidoaki, S., Kwon, I. K., & Matsuda, T. (2005). Mesoscopic spatial designs of nano- and microfiber meshes for tissue-engineering matrix and scaffold based on newly devised multilayering and mixing electrospinning techniques. *Biomaterials*, *26*(1), 37–46. https://doi.org/10.1016/j.biomaterials.2004.01.063

Kilic, I. D., Fabris, E., Serdoz, R., Caiazzo, G., Foin, N., Abou-Sherif, S., & di Mario, C. (2016). Coronary covered stents. *EuroIntervention*, *12*(10), 1288–1295. https://doi.org/10.4244/EIJV12I10A210

Lee, J. H., Kim, E. do, Jun, E. J., Yoo, H. S., & Lee, J. W. (2018). Analysis of trends and prospects regarding stents for human blood vessels. *Biomaterials Research*, *22*(1), 1–10. https://doi.org/10.1186/s40824-018-0114-1

Lei, W. S., Mittal, K., & Yu, Z. (2016). Adhesion measurement of coatings on biodevices/implants: A critical review. *Reviews of Adhesion and Adhesives*, *4*(4), 367–396. https://doi.org/10.7569/RAA.2016.09713

Li, D., & Xia, Y. (2004). Electrospinning of nanofibers: Reinventing the wheel? In *Advanced Materials* (Vol. 16, Issue 14, pp. 1151–1170). https://doi.org/10.1002/adma.200400719

Liang, D., Hsiao, B. S., & Chu, B. (2007). Functional electrospun nanofibrous scaffolds for biomedical applications. In *Advanced Drug Delivery Reviews* (Vol. 59, Issue 14, pp. 1392–1412). https://doi.org/10.1016/j.addr.2007.04.021

McMullin, P. W. (2016). Mechanics of materials. *Introduction to Structures*, 96–125. https://doi.org/10.4324/9781315737737-17

Mitsuo, N., Narushima, T., & Nakai, M. (2015). *Advances in Metallic Biomaterials: Tissues, Materials and Biological Reactions*. 233–250. https://doi.org/10.1007/978-3-662-46842-5

Mittal, B., Mishra, A., Srivastava, A., Kumar, S., & Garg, N. (2014). Matrix Metalloproteinases in Coronary Artery Disease. *Advances in Clinical Chemistry*, *64*, 1–72. https://doi.org/10.1016/B978-0-12-800263-6.00001-X

Morris, B. A. (2017). Effect of Processing on Interlayer Adhesion. In *The Science and Technology of Flexible Packaging*. https://doi.org/10.1016/b978-0-323-24273-8.00015-0

Packham, D. E. (2005). Handbook of Adhesion: Second Edition. In *Handbook of Adhesion: Second Edition* (Vol. 1). https://doi.org/10.1002/0470014229

Petrie, E. M. (2007). An Introduction to Adhesive and Sealants. *Handbook of Adhesives and Sealants*, 896. www.digitalengineeringlibrary.com

Petrie, M. C., Peels, J. O. J., & Jessurun, G. (2006). The role of covered stents: More than an occasional cameo? *Catheterization and Cardiovascular Interventions*, *68*(1), 21–26. https://doi.org/10.1002/ccd.20779

Ramakrishna S, Fujihara K, Teo WE, Yong T, Ma Z, & Ramaseshan R. (2006). Electrospun nanofibers: solving global issues. *Mater Today*, *9*, 40–50.

Schmidt, T., & Abbott, J. (2018). Coronary Stents: History, Design, and Construction. *Journal of Clinical Medicine*, *7*(6), 126. https://doi.org/10.3390/jcm7060126

Xue, J., Xie, J., Liu, W., & Xia, Y. (2017). Electrospun Nanofibers: New Concepts, Materials, and Applications. *Accounts of Chemical Research*, *50*(8), 1976–1987. https://doi.org/10.1021/acs.accounts.7b00218

Yarin, A. L., & Zussman, E. (2004). Upward needleless electrospinning of multiple nanofibers. *Polymer*, *45*(9), 2977–2980. https://doi.org/10.1016/j.polymer.2004.02.066

Zeugolis, D. I., Khew, S. T., Yew, E. S. Y., Ekaputra, A. K., Tong, Y. W., Yung, L. Y. L., Hutmacher, D. W., Sheppard, C., & Raghunath, M. (2008). Electro-spinning of pure collagen nano-fibres - Just an expensive way to make gelatin? *Biomaterials*, *29*(15), 2293–2305. https://doi.org/10.1016/j.biomaterials.2008.02.009

## CURRICULUM VITAE

### Personal Information


Surname, Name : SHAHID, Md Abul
Nationality :
Date of birth and place :
e-mail :


### Education

| Degree | Institution | Graduation Year |
|---|---|---|
| Postgraduate | Cukurova University | 2023 |
| Undergraduate | Bangladesh University of Textiles | 2018 |
| High School | Notre Dame College | 2011 |

### Publications


1) O. Babaarslan, M.A. Shahid, F.B. Do˘gan, Comparative analysis of cotton covered elastomeric hybrid yarns and denim fabric properties, J. Eng. Fiber Fabr. 16 (2021) 155892502110591. Available from: https://doi.org/10.1177/15589250211059188.

2) O. Babaarslan, M.A. Shahid, N. Okyay, Investigation of the performance of cotton/polyester blend in different yarn structures, Autex Res. J. (2022). Available from: https://doi.org/10.2478/AUT-2022-0015.

3) O. Babaarslan, M.A. Shahid, D. Sarapnal, Evaluation of denim fabric performances from sustainable yarn, Mater. Sci. Forum 1063 (2022) 1523. Available from: https://doi.org/10.4028/P-7LBX1O.

4) Babaarslan, Osman, Shahid, Md Abul and Doğan, Fatma B.. "Design of Hybrid Yarn with the Combination of Fiber and Filaments and Its Effect on the Denim Fabric Performance" Fibres & Textiles in Eastern Europe, vol.31, no.1, 2023, pp.25-37. https://doi.org/10.2478/ftee-2023-0004